

Evaluation of hepatic fibrosis: a review from the society of abdominal radiology disease focus panel

Jeanne M. Horowitz,¹ Sudhakar K. Venkatesh,² Richard L. Ehman,² Kartik Jhaveri,³ Patrick Kamath,⁴ Michael A. Ohliger,⁵ Anthony E. Samir,⁶ Alvin C. Silva,⁷ Bachir Taouli,⁸ Michael S. Torbenson,⁹ Michael L. Wells,² Benjamin Yeh,⁵ Frank H. Miller¹

¹Department of Radiology, Feinberg School of Medicine, Northwestern University, 676 St. Clair St, Suite 800, Chicago, IL 60611, USA

²Department of Radiology, Mayo Clinic, 200 First Street SW, Rochester, MN 55905, USA

³Division of Abdominal Imaging, Joint Department of Medical Imaging, University Health Network, Mt. Sinai Hospital & Women's College Hospital, University of Toronto, 610 University Ave, Toronto, ON M5G 2M9, Canada

⁴Division of Gastroenterology and Hepatology, Mayo Clinic, 200 First Street SW, Rochester, MN 55905, USA

⁵Department of Radiology and Biomedical Imaging, UCSF School of Medicine, Zuckerberg San Francisco General Hospital, 1001 Potrero Ave, San Francisco, CA 94110, USA

⁶Department of Radiology, Massachusetts General Hospital, 55 Fruit Street, Boston, MA 02114, USA

⁷Department of Radiology, Mayo Clinic in Arizona, 13400 E. Shea Blvd., Scottsdale, AZ 85259, USA

⁸Department of Radiology and Translational and Molecular Imaging Institute, Icahn School of Medicine at Mount Sinai, 1470 Madison Ave, Box 1234, New York, NY 10029, USA

⁹Department of Laboratory Medicine and Pathology, Mayo Clinic, 200 First Street SW, Rochester, MN 55905, USA

Abstract

Hepatic fibrosis is potentially reversible; however early diagnosis is necessary for treatment in order to halt progression to cirrhosis and development of complications including portal hypertension and hepatocellular carcinoma. Morphologic signs of cirrhosis on ultrasound (US), computed tomography (CT), and magnetic resonance imaging (MRI) alone are unreliable and are seen with more advanced disease. Newer imaging techniques to diagnose liver fibrosis are reliable and accurate, and include magnetic resonance elastography and US elastography (one-dimensional transient elastography and point shear wave elastography or acoustic radiation force impulse imaging). Research is ongoing with multiple other techniques for the noninvasive diagnosis of hepatic fibrosis, including MRI with diffusion-weighted imaging, hepatobiliary contrast enhancement, and perfusion; CT using perfusion, fractional extracellular space techniques, and dual-energy, contrast-enhanced US, texture analysis

in multiple modalities, quantitative mapping, and direct molecular imaging probes. Efforts to advance the non-invasive imaging assessment of hepatic fibrosis will facilitate earlier diagnosis and improve patient monitoring with the goal of preventing the progression to cirrhosis and its complications.

Key words: Chronic liver disease—Fibrosis—Elastography—Magnetic resonance imaging—Sonography—Perfusion

The diagnosis and staging of hepatic fibrosis has become extremely important in clinical decision making. Accurate staging of fibrosis and appropriate treatment in certain etiologies (such as chronic hepatitis B and C) may reverse or prevent the progression to advanced cirrhosis and its potential complications including hepatocellular carcinoma (HCC) and portal hypertension. Hepatic fibrosis can develop in patients with any chronic liver disease (CLD), including hepatitis C, hepatitis B, alcoholic liver disease, nonalcoholic fatty liver disease (NAFLD), and autoimmune hepatitis. The progression

from hepatic fibrosis to cirrhosis is generally slow, taking place over decades in conditions such as HCV infection or NASH, but can occur more rapidly in the presence of biliary obstruction, immunosuppression in post-liver transplant patients, or with human immunodeficiency virus (HIV) co-infection [1–3]. If hepatic fibrosis is diagnosed at an early stage, it can be treated and reversed with weight loss in nonalcoholic steatohepatitis (NASH) and anti-viral therapy for hepatitis B or C infections. [4]. Therapy will hopefully reduce morbidity and mortality of CLD and its complications. However, fibrosis and cirrhosis of the liver will continue to be a major clinical concern even with successful treatment of hepatitis C.

Hepatic fibrosis is a response to chronic inflammation and hepatocyte injury. The liver parenchyma heals by laying down more collagen fibers in the extracellular matrix (ECM). Normally, collagen comprises less than 1% of the liver but this amount increases several fold in CLD [5, 6]. Hepatic fibrosis results in both quantitative and qualitative changes in the collagen and noncollagenous components of the ECM [7]. Fibrosis is a dynamic process of deposition of excessive collagen fibers balanced with degradation and remodeling [8]. When the accumulation of collagen fibers exceeds degradation, fibrosis progression to cirrhosis may result. A response to treatment results in the reduction in fibrosis content, which is typically a slow process extending over months to years.

Traditionally, the diagnosis of hepatic fibrosis and determination of fibrosis stage was made using liver biopsy. Liver biopsy can also provide important information about the etiology of CLD, in patients with unexplained elevated liver function tests. However, liver biopsy is not the optimal method for diagnosis and fibrosis staging in all patients because of poor patient acceptance and small risk of complications. Also serial liver biopsies are not practical for frequent or long-term monitoring of a patients' response to treatment. In addition, liver biopsy results are variable due to sampling errors related to both small sample size and spatial variation in degree of fibrosis and variability of pathologist interpretation [9, 10]. A recent study reported a difference of at least one fibrosis stage in 30% of series of 111 biopsy specimens evaluated by different pathologists [11]. While liver biopsies remain as an important clinical tool, modern medical management of liver disease often relies on regular interval assessments of liver fibrosis. Many noninvasive techniques are now available and have become an important part of patient care and may potentially replace liver biopsy. The noninvasive imaging techniques used to diagnose liver fibrosis will be discussed in detail in this paper.

Histologic evaluation of hepatic fibrosis

Multiple histologic scoring systems for hepatic fibrosis are applied to liver histology specimens. The system used

depends on the etiology of chronic liver disease. Common to all of these systems are these four basic fibrosis stages: no fibrosis, portal/periportal fibrosis, bridging fibrosis, and cirrhosis. The different staging systems vary largely in how these stages are subdivided. For example, the Ishak system divides portal fibrosis into mild and moderate, while the METAVIR system does not. Also of note, steatohepatitis and vascular outflow disease also have an additional fibrosis stage, typically located between no fibrosis and portal fibrosis, which is characterized by pericellular and/or central vein fibrosis [12, 13]. Histological fibrosis staging systems are based fundamentally on architectural changes. Thus, the different fibrosis stages are not “additive” in the strictly mathematical sense. As examples, stage 1 fibrosis does not necessarily have half of the collagen of stage 2, and stage 4 does not have twice the collagen of stage 2. Fibrosis progression is also not uniform over time, with fibrosis tending to progress more slowly in early stages with small incremental increase in collagen content as compared to exponential increase in collagen content during later stages [14–16].

The most common scoring systems used for clinical care include the modified histology activity index (also called the Ishak system) [17], the METAVIR system [18], and the Batts–Ludwig system [19]. Scoring systems also exist for specific liver diseases, including nonalcoholic fatty liver disease [13], alcoholic hepatitis [20], primary biliary cirrhosis [21], and primary sclerosing cholangitis [22]. In addition, subclassifications of cirrhosis have been developed (based on nodule size and septal fibrosis thickness) which have shown potentially useful correlations with severity of portal hypertension and other clinical complications [23–27]. Histologic scoring of both necroinflammatory activity (grade of injury) and the degree of fibrosis (fibrosis stage) helps predict the response of fibrosis to treatment. Many noninvasive imaging tests attempt to predict the five-point METAVIR histologic score of F0–F4, where $\geq F2$ is clinically significant fibrosis, $\geq F3$ is advanced fibrosis, and F4 is cirrhosis. This score helps predict the response of fibrosis to treatment, since F3 and F4 patients are considered advanced stage and less likely to respond, and determines if the patient has cirrhosis and requires screening for HCC.

Quantitative measurements of collagen can also be used to measure small changes in total fibrosis content. Among these, the collagen proportionate area is considered to be the most accurate. It has been studied in many patient populations and successfully used to measure response to treatment [14, 28, 29]. The drawbacks are that it still requires a liver biopsy and correlates poorly with clinical staging systems. However, this methodology is still useful in drug trials and at institutions where specialized liver clinics are present.

Noninvasive tests

Noninvasive assessment of hepatic fibrosis can be done with serologic tests or imaging. Serologic testing is desirable because of its noninvasive nature and potential wide availability. Serologic tests for liver fibrosis include direct and indirect assessments of liver fibrosis. The direct tests detect byproducts of degradation or synthesis of collagen. The indirect tests assess the effect of fibrosis on function of hepatocytes.

These tests include the serum aspartate aminotransferase-to-platelet ratio index, FibroTest (BioPredictive, Paris, France)/FibroSure (LabCorp, Burlington, NC, USA), Hepascore (Quest Diagnostics), FIBROSpect (Prometheus Corp), and the European Liver Fibrosis Study Group panel (not available in the United States). Unfortunately, serum tests are not reliable because inflammation outside of the liver can contribute to false-positive test results, and serum levels are affected by clearance rates, which may be impaired due to sinusoidal endothelial cell dysfunction or impaired biliary excretion. The serum panels also cannot distinguish between different levels of fibrosis, although serum markers do work well for diagnosing advanced fibrosis and cirrhosis. Serum markers can differentiate patients with significant fibrosis (F2–F4) from those without significant fibrosis (F0–F1) with fair to good accuracy (AUROC 0.70–0.86) [30]. Indeterminate outcomes are common, in one study serum markers could rule-in or rule-out fibrosis in only 35% of patients [31]. Indirect markers of fibrosis which have been combined into serologic panels include serum aminotransferase levels, platelet count, coagulation parameters, gamma-glutamyl transferase (GGT), total bilirubin, alpha 2 macroglobulin, and alpha 2 globulin (haptoglobin). In a meta-analysis of 86 studies including 19,533 patients assessing how to diagnose cirrhosis through laboratory tests and physical exam, the presence of ascites, a platelet count $< 160 \times 10^3/\mu\text{L}$, spider nevi, or a combination of simple laboratory tests with the Bonacini cirrhosis discriminant score > 7 were the most reliable [32].

Diagnosing liver fibrosis with imaging

Hepatic fibrosis has traditionally been diagnosed at imaging by assessment of morphologic abnormalities on ultrasound (US), computed tomography (CT), and magnetic resonance imaging (MRI). Novel imaging techniques used to diagnose liver fibrosis and cirrhosis available in clinical practice include US elastography and MR elastography. Other imaging methods of diagnosing liver fibrosis are currently of research interest with potential clinical application and include diffusion-weighted imaging, MRI with hepatobiliary contrast agents, MR and CT perfusion, dual-energy CT, contrast-enhanced US, image texture analysis, and direct molecular imaging probes of collagen.

Morphologic assessment

Morphologic features of cirrhosis can be assessed on US, CT, or MRI (Fig. 1A–F), and include an atrophic right lobe and segment IV, hypertrophy of the caudate and lateral left lobes, liver surface nodularity, a right hepatic posterior notch, an expanded gallbladder fossa, narrow hepatic veins < 5 mm, an enlarged caudate to right lobe ratio (> 0.90), and enlargement of the hilar periportal space > 10 mm [33–45]. The sensitivity, specificity, accuracy, and positive predictive value of some of these morphologic features of cirrhosis are shown in Table 1 [33–35, 37–39, 41–45]. While these morphologic features are fairly good at diagnosing cirrhosis, they suffer from low sensitivity and are not always present at earlier stages of fibrosis. Although some of these morphologic features are semiquantitative, many are subjective. This leads to expected interobserver variability found within studies and variable measures of accuracy reported between studies.

Radiologists should be cautious about diagnosing or excluding cirrhosis using these morphologic features. For example, in one study, 15% of patients with advanced fibrosis/cirrhosis on liver biopsy (F3–F4) and elevated stiffness on MR elastography showed normal morphologic features on conventional MRI [46]. Another study showed 20% or more patients with cirrhosis and elevated liver stiffness on MR elastography had no morphological features of cirrhosis on conventional MRI [47].

Grayscale and Doppler ultrasound

Conventional B mode or “grayscale” US is widely used as a first-line imaging modality in evaluation of patients with liver disease because it is widely available, has no known adverse bioeffects, is inexpensive, and has reasonable sensitivity for the detection of focal liver lesions, cholelithiasis, and biliary ductal dilatation. In one study, cirrhosis could be correctly diagnosed on US in 82–88% of patients with CLD using a few signs detected on conventional US, including spleen length, portal velocity, liver surface, and liver length [48]. Unfortunately, conventional US is known to have significant interoperator variability. In a meta-analysis of 21 studies of diagnostic US in CLD, wide variation in the reported diagnostic sensitivities and specificities for liver fibrosis and cirrhosis was observed [49]. Similarly, while a heterogeneous or coarsened liver echotexture is associated with cirrhosis [50, 51], the diagnosis of hepatic heterogeneity is inherently subjective. Moreover, the US appearance of hepatic cirrhosis and steatosis can be similar, producing a “fatty-fibrotic” pattern [51, 52]. Measurements of liver echogenicity have shown poor predictive accuracy for the diagnosis of fibrosis [53, 54]. Due to decreased penetration of the US beam, hepatic evaluation is limited in

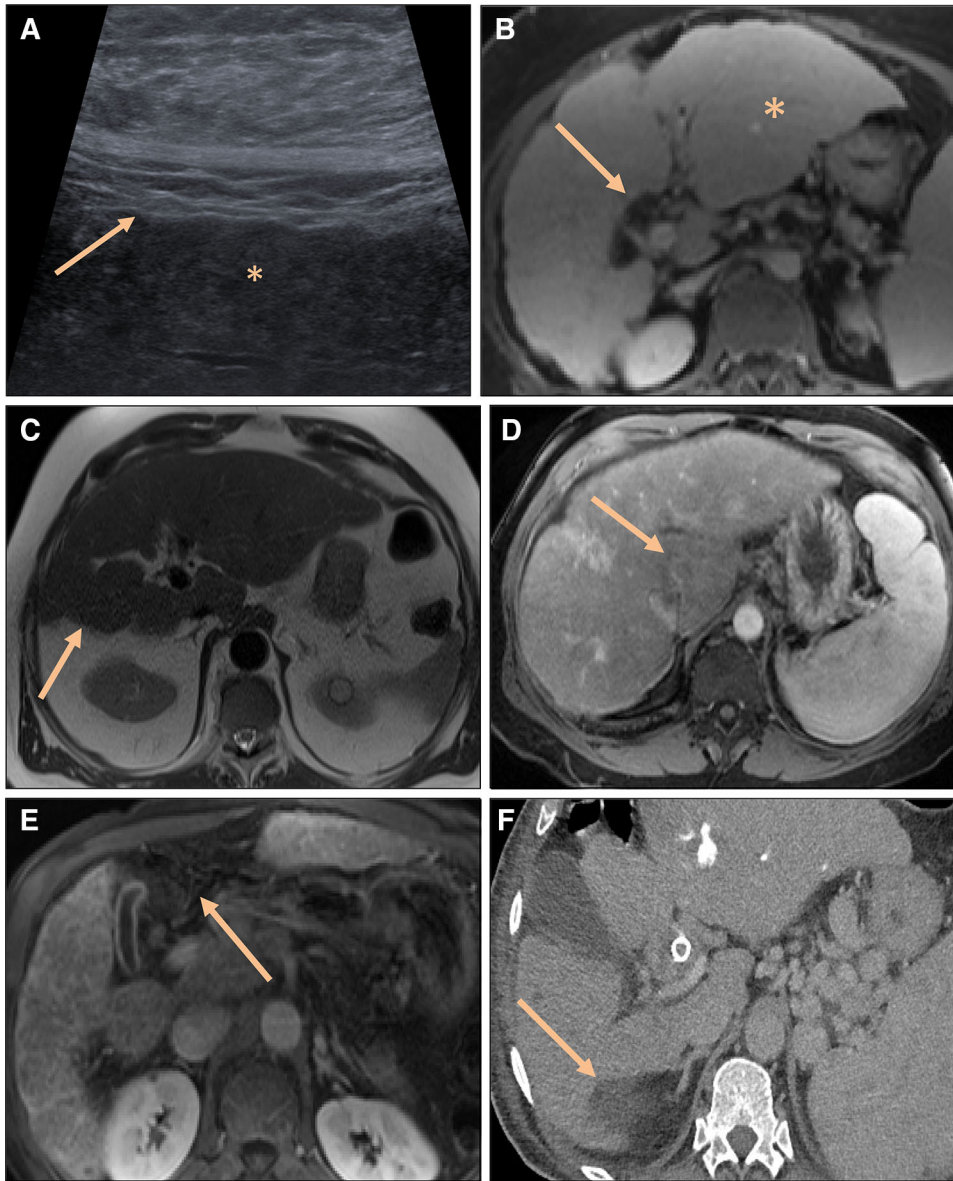


Fig. 1. A–F Morphologic imaging features of cirrhosis in 6 patients. (A) Ultrasound shows a nodular surface (arrow) and coarsened echotexture (asterisk). MRI images of cirrhotic livers show (B) a nodular surface contour, hypertrophy of lateral left lobe (asterisk), and expanded hilar periportal space (arrow) on post-contrast T1 FS sequence, (C) atrophic right hepatic lobe (arrow) on axial T2 Half-Fourier Acquisition Single-Shot Turbo Spin-Echo (HASTE) sequence, (D) hypertrophy of caudate lobe on post-contrast T1 FS sequence (arrow), (E) expanded gallbladder fossa and atrophic medial segment left lobe on post-contrast T1 FS sequence (arrow). (F) Post-contrast CT in the portal venous phase shows a right hepatic posterior “notch” (arrow).

Table 1. Morphologic features of cirrhosis

| Feature | Se | Sp | Accuracy | PPV |
|--|-------|-------|----------|-----|
| Surface nodularity | 91.8% | 84.3% | 88.0% | |
| Right posterior “Notch” | 72% | 98% | 82% | 99% |
| Expanded gallbladder fossa | 68% | 98% | 80% | 98% |
| Narrow right hepatic vein (<5 mm) | 59% | 99% | | |
| Caudate to right lobe ratio (>0.90) | 71.7% | 77.4% | 74.2% | |
| Expanded hilar periportal space (>10 mm thickness) | 93% | 92% | 92% | 91% |

obese patients, making detection of cirrhosis and liver lesions difficult.

Color Doppler US can aid in diagnosing portal flow abnormalities associated with cirrhosis, including slow or hepatofugal portal venous flow [55]. However, these flow abnormalities are not seen in the early fibrosis stages.

Spectral Doppler US showing decreased phasicity of the hepatic venous waveforms can be seen in hepatic fibrosis and steatosis [56, 57]. In general, evidence suggests that Doppler US measurements of the portal vein, hepatic artery, and hepatic veins should not be used to stage liver fibrosis [58].

US elastography

US elastography measures liver stiffness by measuring the velocity of acoustically induced mechanical shear waves propagating through the liver, a process termed shear wave elastography. The speed of shear waves traveling through the liver is faster in stiffer fibrotic livers than in normal livers. A number of proprietary elastography technology embodiments have been developed by different manufacturers of elastography equipment, including acoustic radiation force impulse imaging (ARFI) and dynamic shear wave elastography (SWE).

Transient elastography (TE) is performed with Fibroscan (Echosens, Paris, France). TE is the most validated method of US elastography for the noninvasive diagnosis of liver fibrosis. In TE, a single element transducer generates a short duration transient vibration which generates a shear wave that propagates longitudinally with respect to the transducer axis [59]. Advantages of TE include that TE can be used by physicians at the bedside and is inexpensive and portable [59]. TE, however, is not an imaging technique and does not display the location where stiffness is measured to confirm that it is in fact in the liver. TE cannot evaluate liver parenchyma for hepatic disease or masses. [59].

A number of meta-analyses have assessed the performance of TE for diagnosing hepatic fibrosis [60–63]. Stiffness cutoff values for hepatic fibrosis of \geq F2, F3, and F4 from these meta-analyses are 7–7.65, 9.5, and 12–13.01 kPa, respectively (AUC 0.84–0.8701 for \geq F2, 0.89 for \geq F3, and 0.93–0.96 for \geq F4) [60–64]. Commonly used cutoff values for TE in clinical practice are >7 kPa for significant fibrosis ($>$ F2) and >11 –14 kPa for cirrhosis in chronic hepatitis C patients [65]. However, the cutoff values used for cirrhosis in chronic hepatitis B patients are lower than hepatitis C at 9–10 kPa [66], and research is ongoing with regards to differences in cutoff values for various other underlying etiologies for hepatic fibrosis. It should be noted that the cutoff values are different between TE and MR elastography because values in TE are based on the bulk modulus or Young's Modulus (E) and MR elastography on "magnitude of the complex shear modulus" (μ) (E being $\sim 3 \times (\mu)$). Similar to imaging-based US techniques, TE has an excellent negative predictive value for cirrhosis [60–64, 67] and intermediate accuracy for distinguishing between intermediate fibrosis stages [68].

TE is less reliable in patients with obesity, narrow intercostal spaces, and/or ascites. An "XL" TE probe is now available for examining obese patients. Nonetheless, the failure rate of TE ranges from 6% to 23% [59, 69–71].

Imaging-based US shear wave elastography can be more readily used in patients with obesity, ascites, and NAFLD [72–74]. The site of liver stiffness measurement is saved on the images and can be used in follow-up measurements when monitoring patients undergoing

treatment for hepatic fibrosis. In patients with cirrhosis, HCC screening can be performed with US at the same examination.

In ARFI US, acoustic compression pulses are focused inside the liver, and some of the acoustic energy is absorbed and released as shear waves traveling perpendicular to the US beam [59]. Several meta-analyses have studied the performance of ARFI in the diagnosis of hepatic fibrosis [60, 75, 76]. Velocity cutoff values for hepatic fibrosis of \geq F2, \geq F3, and F4 from these meta-analyses are 1.30–1.34, 1.55, and 1.8 m/s, respectively [60, 64, 75, 76]. These meta-analyses of ARFI-based liver fibrosis staging show for hepatic fibrosis of \geq F2 an AUC 0.85–0.87; \geq F3 an AUC 0.91; and F4 an AUC 0.93 [60, 64, 75, 76]. In a meta-analysis comparing TE and ARFI, inability to obtain reliable measurements was more than 3 times as high for TE as ARFI (6.6% vs. 2.1%, $P < 0.001$) [60].

2D Shear wave elastography (SWE) (Supersonic Imagine, Aix-en-Provence, France) is another technique that uses focused acoustic energy to generate shear waves in a manner similar to ARFI, but captures the propagation of shear waves in real time. Having multiple regions of interest reduces sampling variability compared with TE and ARFI [77]. In one meta-analysis, cutoff values and AUC for 2D SWE for stage \geq F1, \geq F2, \geq F3, and F4 fibrosis were 7.1 kPa and 0.825, 7.8 kPa and 0.859, 8 kPa and 0.897, 11.5 kPa and 0.914, respectively [78]. The performance of this type of shear wave elastography is promising [77–81], but is not as widely validated as TE or ARFI-based approaches.

ARFI and 2D SWE measurements should be made 1–3 cm deep to the liver capsule to reduce artifacts [82]. Measurements should preferably be made intercostally in the right lobe, which has been shown to be more accurate than left lobe measurements [75, 83]. Measurements should be acquired during shallow breath holding or resting expiration to minimize liver motion, as deep inspiration increases stiffness measurements compared with resting expiratory position [84]. Figure 2A, B shows an example of liver fibrosis identified with ARFI which was not detectable with conventional grayscale US.

Patients undergoing US elastography should be fasting [85, 86]. Liver stiffness measurements on elastography can be influenced not only by fibrosis, but also edema, inflammation [87], alcohol use, extrahepatic cholestasis [88], hepatic congestion [89], and operator inexperience, and it is therefore important for the interpreting radiologist to be cognizant of these pitfalls, and to review the medical record to the extent possible.

Magnetic resonance imaging

While MRI is not as readily available as US, advantages include less operator dependence and more accurate evaluation of patients with NAFLD. MRI can assess for

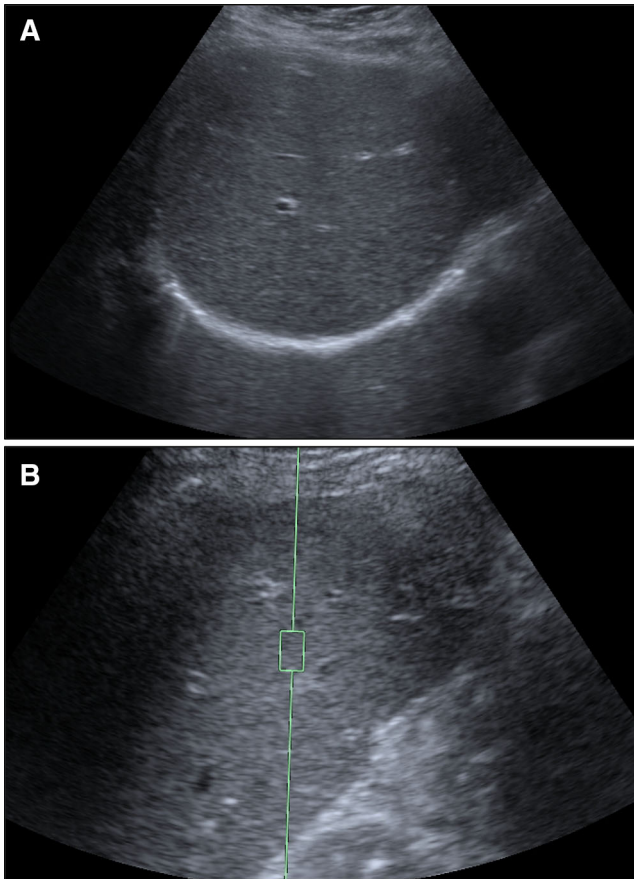


Fig. 2. A, B Ultrasound of a 61-year-old woman with HIV and hepatitis C presenting for fibrosis screening shows potentially treatable liver fibrosis on ARFI prior to morphologic changes on grayscale ultrasound. **(A)** Grayscale ultrasound of the right hepatic lobe shows a normal smooth echotexture. **(B)** ARFI shows a shear wave velocity of 1.79 m/s (F3).

morphologic features of cirrhosis, and advanced fibrosis can be seen on dynamic contrast-enhanced (DCE) T1-weighted imaging sequences. Fibrotic bands appear as linear areas of high T2 signal and portal venous phase enhancement (Fig. 3A, B). Earlier stages of fibrosis will not be seen on conventional contrast-enhanced MRI. Texture analysis can also be performed on MRI, which will be discussed later.

Magnetic resonance elastography

Magnetic resonance elastography (MR elastography) is the currently most accurate noninvasive technique for detection and staging of liver fibrosis [90–92]. Several studies have demonstrated that the diagnostic performance of MR elastography in this role is superior to that of TE and ARFI [92, 93]. In particular, MR elastography is notable for its ability to accurately diagnose mild fibrosis which is difficult using other imaging techniques, including TE [51]. MR elastography results are highly reproducible and have excellent interobserver agreement,

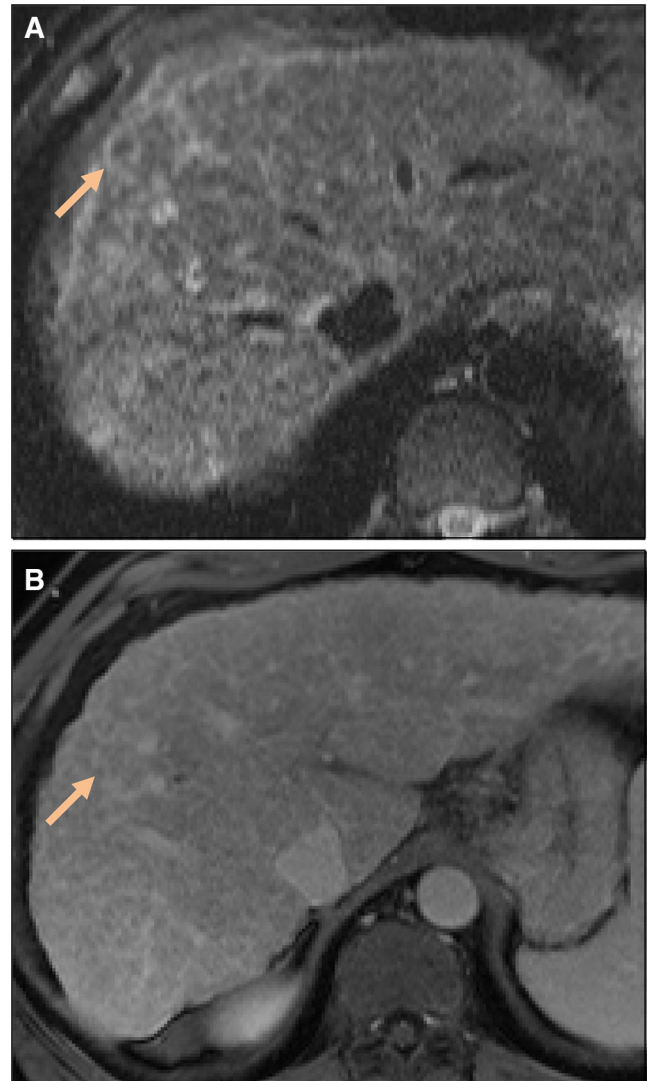


Fig. 3. A, B Bands of linear hepatic fibrosis on MRI are **(A)** T2 hyperintense on T2 FS sequence and **(B)** show delayed enhancement.

due in part to the large volume of liver assessed which limits sampling error [92, 94–97] and better than morphological features to diagnose cirrhosis [46, 92]. The elastogram also allows characterization of the regional distribution of fibrosis in the liver which may be useful for diagnosing underlying liver disease such as primary sclerosing cholangitis.

MR elastography requires a driver to generate mechanical shear waves in the liver. An acoustic wave generator is placed outside the scanner room. Beneath the surface coil arrays, a disk-shaped, passive driver is placed against the right lower chest/upper abdomen along the mid clavicular line at the level of the xiphoid process [90]. Acoustic pressure waves are conducted from the wave generator to the passive driver via a long, flexible, plastic tube [90]. Pulse sequences with motion encoding gradients are used to visualize traversing shear

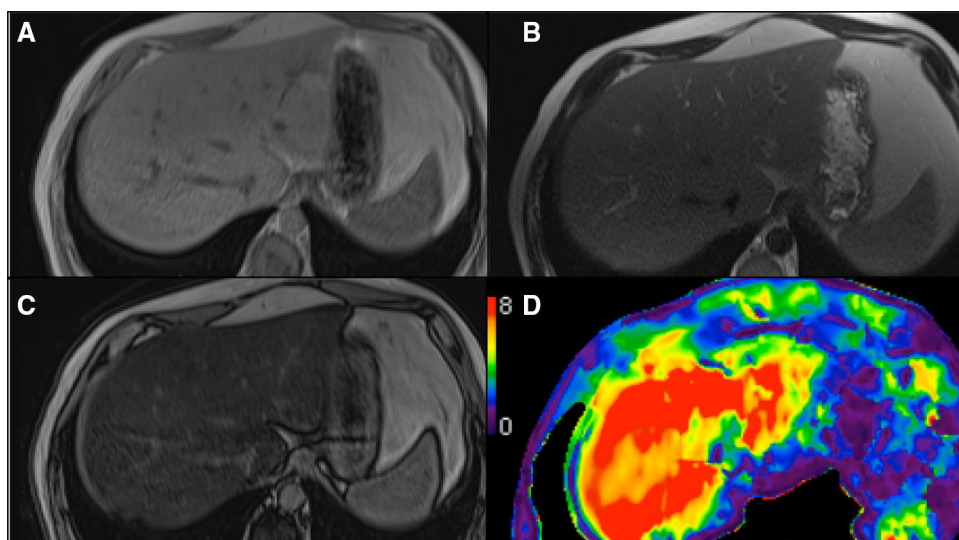


Fig. 4. A–D A 57-year-old man with fatty liver disease. Hepatic steatosis is seen with signal loss on the opposed phase imaging relative to the in phase images (**A** and **C**), but with normal liver morphology on T1- and T2-weighted imaging (**A–C**). (**D**) MR elastography shows unsuspected cirrhosis (stiffness 7.5 kPa), making biopsy unnecessary.

waves; these sequences can be designed with gradient-recalled echo, spin-echo, balanced steady-state free precession, or echo-planar imaging (EPI) technique [90]. The phase-sensitive MR images are then processed by an inversion algorithm to create wave images and quantitative elastogram images depicting tissue stiffness. The elastograms are analyzed by manually drawing regions of interest or by using automated segmentation [59, 90]. The regions of interest should exclude liver edge, fissures, gallbladder fossa, lesions, and large vessels. The average stiffness from several slices is reported as the mean stiffness value in kilopascals (kPa). An example of MR elastography imaging is shown in Fig. 4A–D.

Stiffness cutoff values for hepatic fibrosis \geq stage F2, F3, and F4 from an MR elastography meta-analysis were 3.66, 4.11, and 4.71 kPa respectively [92]. Two meta-analyses studying the performance of MR elastography show for hepatic fibrosis of \geq F2 an AUC 0.88–0.98, sensitivity 0.79–0.94, and specificity 0.81–0.95; F3 an AUC 0.93–0.98, sensitivity 0.85–0.92, and specificity 0.85–0.96; and F4 an AUC 0.92–0.99, sensitivity 0.91–0.99, specificity 0.81–0.94 [92, 98].

Compared with US elastography, MR elastography performs better for diagnosing fibrosis in obese patients and patients with ascites, with fewer nondiagnostic cases and is able to detect fibrosis throughout the liver. Contrast-enhanced MRI can also diagnose HCC when performed in the same setting as MR elastography [92]. The diagnostic capability of MR elastography is less affected by obesity, whereas with US elastography, unreliable measurements were found in 35.4% of TE exams in obese patients [99] and 17.6% of ARFI exams in obese patients [100]. MR elastography has shown a higher technical success rate compared with TE, 94% vs. 84% [101].

MR elastography has been validated in various underlying etiologies of cirrhosis, including chronic hepatitis B, chronic hepatitis C, and NAFLD [102–104].

Most studies have indicated that steatosis does not have significant effect on MR elastography assessed liver stiffness [96, 97, 105], although obesity can play a small role in MR elastography failure [106]. Liver stiffness may be elevated in the absence of significant fibrosis in patients with acute alcohol intoxication, acute hepatitis, acute flares of chronic hepatitis, biliary obstruction, chronic inflammation, and passive congestion due to cardiac failure or other cardiac conditions. The results of MR elastography exams should be interpreted taking into account such co-existing conditions.

MR elastography has some limitations. The current clinical MR elastography sequence (2D GRE) may fail in patients with moderate-to-severe hepatic iron deposition [101], contributing to a failure rate in one meta-analysis of 4.3% [92]. Another recent study showed the technical failure rate of MR elastography at 1.5 T was 3.5%, with independent risk factors associated with failure of MR elastography including massive ascites, iron deposition, and high body mass index [106]. This limitation from iron deposition is secondary to the low parenchymal signal; however, the shear waves still traverse through the liver but are not visualized as liver parenchyma does not have enough signal intensity for post-processing by the inversion algorithm. Better technical success in patients with hepatic iron deposition may be obtained by using pulse sequences with shorter echo times such as spin-echo EPI based MR elastography [91, 107]. MR elastography may also be limited in patients who cannot hold their breath. Breath holding time can be reduced by decreasing the field of view or reducing the matrix size at the cost of resolution in order to obtain more accurate results [90]. Similar to US elastography, patients should be fasting 4–6 h prior to MR elastography, since a post-prandial state increases liver stiffness in patients with fibrosis or cirrhosis [108, 109].

Noninvasive diagnosis of liver fibrosis: Imaging techniques of research interest

While US elastography, including TE and point SWE/ARFI, and MR elastography are clinically available and validated as noninvasive means of diagnosing liver fibrosis, several other imaging techniques show promise in their ability to noninvasively diagnose liver fibrosis but are primarily of research interest at this time, and clinical translation is still awaited. These include MRI techniques including diffusion-weighted imaging, MRI with hepatobiliary contrast, MR perfusion, and quantitative T1, T2, T1 rho mapping; CT techniques including perfusion, fractional extracellular space, and dual-energy/spectral CT; contrast-enhanced US, texture analysis, and direct molecular imaging probes of collagen.

Diffusion weighted imaging (DWI)

DWI can be used to diagnose fibrosis and cirrhosis on MRI exams. Hepatic fibrosis causes restricted diffusion that can be quantitatively measured with the hepatic apparent diffusion coefficient (ADC) value. Lower ADC values in advanced stages of hepatic fibrosis may be related to the presence of increased connective tissue in the liver combined with decreased blood flow [110], or possibly due to diminished hepatic perfusion in cirrhotic patients rather than decreased extravascular diffusion [111–113]. An example of lower ADC in a cirrhotic patient is shown in Fig. 5.

DWI is better at distinguishing between cirrhotic and normal livers than distinguishing between stages of fibrosis [98, 114]. One study showed a positive predictive value, negative predictive value, and overall accuracy of 100%, 99.9%, and 96.4%, for diagnosing cirrhosis compared with controls [115]. DWI does not perform as well as MR elastography [98, 116, 117]. In comparative study, MR elastography demonstrated higher sensitivity and specificity in predicting fibrosis scores $\geq F2$ (91% and 97%), $\geq F3$ (92% and 95%), and F4 (95% and 87%) compared with DWI (84% and 82%, 88% and 76%, and 85% and 68%, respectively) [117]. Similarly, a meta-analysis showed DWI distinguishing F0–F1 from F2–F4 with a sensitivity of 77%, specificity of 78%, and AUC of 0.83; less reliable than MR elastography [98]. A more recent study showed that for detection of advanced fibrosis (F3–F4), AUCs were 0.94 for MR elastography and 0.79 for DWI [116].

DWI image quality can suffer particularly in patients with cirrhosis and ascites. Other limitations for using DWI are that ADC values are dependent on the particular MRI scanner, the b -values used, and whether breathhold or free breathing techniques are employed, and so published ADC results are not generalizable to all scanners. DWI signal is also affected by hepatic iron deposition [118].

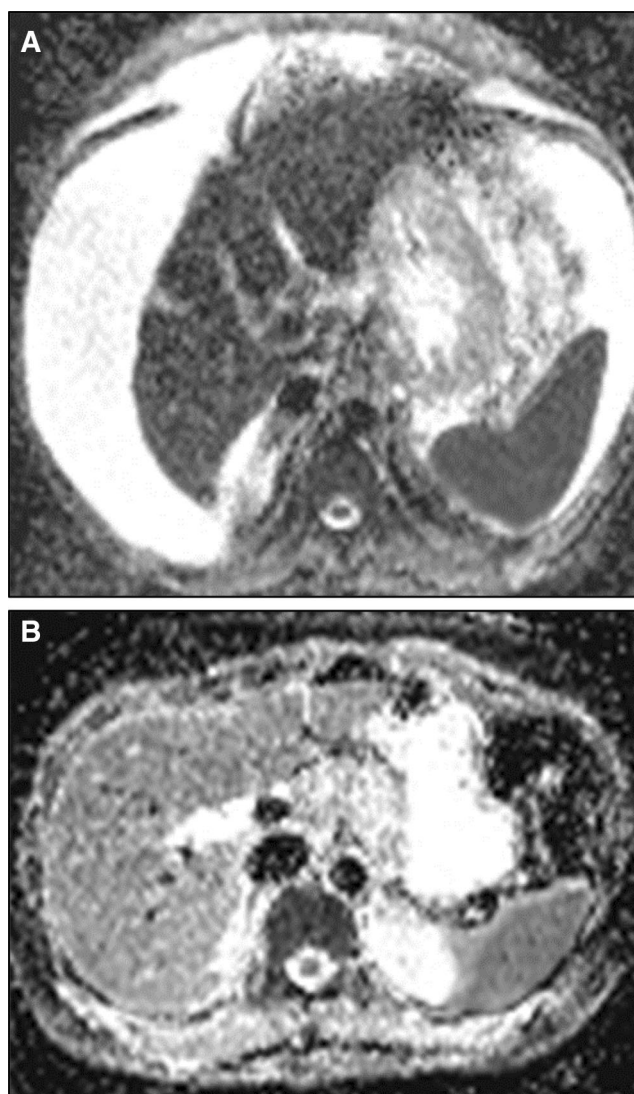


Fig. 5. **A, B** ADC maps from MRI with DWI show lower ADC in a cirrhotic patient (**A**) compared with a patient without chronic liver disease (**B**).

Intravoxel incoherent motion (IVIM) DWI assesses diffusion and perfusion by acquiring multiple b -values, and by processing the data using a bi-exponential model [113, 119, 120]. IVIM has shown potential in staging hepatic fibrosis [120–125]. One study showed that both IVIM and ARFI provide reliable estimations for the noninvasive assessment of liver fibrosis [125]. However, another study showed that IVIM imaging does not discriminate fibrosis stages as well as MR elastography [123].

MRI with hepatobiliary contrast agents

Hepatobiliary MRI contrast agents: gadoxetate disodium (Eovist/Primovist; Bayer Healthcare, Wayne, NJ) and gadobenate dimeglumine (MultiHance; Bracco

Diagnostics, Princeton, NJ) play a well-established and important incremental role in liver lesion detection and characterization [126, 127] in addition to routine extracellular contrast agents. After intravenous injection, gadoxetate disodium is taken up by hepatocytes and approximately 50% is excreted through the bile ducts, while gadobenate dimeglumine shows only approximately 5% biliary excretion. The degree of hepatic uptake and biliary excretion of these contrast agents has been investigated as a surrogate biomarker for estimation of liver function and diffuse liver disease. There has been growing and significant interest in the ability of gadoxetic acid-enhanced liver MRI for staging liver fibrosis since some of the earlier work in animal models and humans [128–132]. Since then a number of studies have been published showing the ability of gadoxetic acid uptake as a surrogate marker to stage liver fibrosis including some comparisons against DWI, aspartate aminotransferase-to-platelet ratio index, Fib-4, US, and MR elastography [133–139].

The underlying principles for staging hepatic fibrosis with gadoxetic acid essentially rely on MRI-based quantification of decreased hepatic enhancement on hepatobiliary phase images (Fig. 6). This is caused by either reduced hepatic uptake associated with decreased expression of the hepatic organic anion transporters due to either decrease in normal hepatocytes or hepatocyte dysfunction, degeneration or necrosis, and/or prolongation of liver enhancement due to decreased biliary excretion with increasing hepatic fibrosis [130, 140]. Hepatic uptake of gadoxetate disodium is dependent on specific cellular transporters (OATP receptors). Normal variants of the OATP receptors in the population may decrease hepatic enhancement by 30–40% and represent a confounding factor for interpretation of gadoxetate disodium uptake studies [141].

The quantitative indices utilized in published work include contrast enhancement index (CEI), relative liver enhancement (RLE) and T1 mapping of hepatobiliary phase images. CEI is calculated as $SI_{\text{post}}/SI_{\text{pre}}$, where SI_{post} and SI_{pre} are, respectively, the liver-to-muscle signal intensity ratio on hepatobiliary phase images and on unenhanced images while RLE is calculated as $(SI_{\text{post}} - SI_{\text{pre}})/SI_{\text{pre}}$. T1 mapping involves measuring the T1 relaxation time of liver tissue and correlates directly with gadoxetic acid contrast concentration at time of hepatobiliary phase acquisition. Initial work by Watanabe et al. [130] reported CEI to be an accurate biomarker for staging liver fibrosis compared to other enhancement indices as well as hematological markers and DWI. CEI was also more significantly correlated with fibrosis stage than it was with necroinflammatory activity grade. Subsequently, Choi et al. [138] found significant correlation between CEI and histologic staging of hepatic fibrosis. However, MR elastography showed higher sensitivity and specificity for predicting hepatic fibrosis

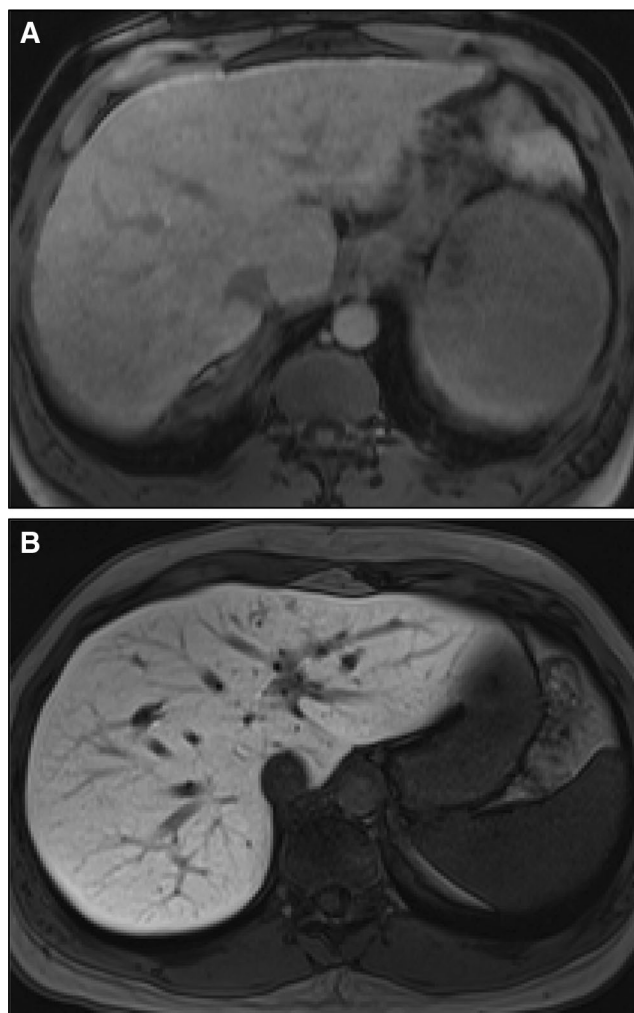


Fig. 6. A, B MRI using hepatobiliary contrast shows that on the hepatocyte phase, there is decreased liver enhancement of a cirrhotic liver (A) compared with a noncirrhotic liver (B).

stages F2 (87% and 91%), F3 (80% and 89%), and F4 (81% and 85%) compared with CEI (46% and 82%, 63% and 68%, and 76% and 65%, respectively). Similarly, Park et al. [135] have reported strong correlation between liver stiffness (MR elastography) and APRI, while CEI and ADC showed weak or negative correlation in patients with liver fibrosis. RLE has been shown to demonstrate good accuracy for detecting moderate-to-advanced fibrosis (>F2) and cirrhosis (F4) [142].

A few studies have investigated T1 mapping of gadoxetic acid-enhanced liver MRI in fibrosis staging and correlation with hepatic molecular transporters. Published work [134] has revealed that T1 relaxation time obtained from hepatobiliary phase image is significantly correlated with the fibrosis stage with high diagnostic accuracy for stage 3 fibrosis (AUROC of 0.82), a relatively low diagnostic accuracy for grade 3 necroinflammatory activity (AUROC of 0.68), and significantly higher accuracy than DWI-ADC values for liver fibrosis

staging. However, in another study [137] US elastography was found to be superior to T1 relaxation time measurement in differentiating stage \geq F2.

More recently published studies have suggested that the gadoteric acid-enhanced T1 relaxation time index appears to be superior to APRI and FIB-4 for predicting hepatic fibrosis and the combined use of gadoteric acid-enhanced T1 mapping, APRI, and FIB-4 may be more reliable for staging liver fibrosis in chronic hepatitis B and can be regarded as a useful imaging biomarker of hepatocyte transporter function [143, 144].

Despite a good body of evidence supporting role of gadoteric acid liver MRI in detecting and staging liver fibrosis, its clinical utilization is essentially negligible in most centers and awaits translation from the research arena into the clinical realm.

MR perfusion

Assessing liver fibrosis with MR perfusion (DCE-MRI) has also been studied in recent years and is mostly of research interest currently. Three-dimensional gradient-recalled-echo sequence performed with parallel imaging allows evaluation of liver perfusion with high temporal resolution [145], although perfusion analysis is relatively labor intensive. Arterial blood flow, arterial fraction, portal venous fraction, distribution volume, and mean transit time in one study were significantly different between patients with and without severe fibrosis [145]. Distribution volume of at least 21% had the best performance in this study, with an AUC 0.824, 76.9% sensitivity (95% confidence interval: 46.2%, 94.7%), and 78.5% specificity (95% confidence interval: 49.2%, 95.1%) in the prediction of F3-advanced fibrosis [145].

In a recent prospective study comparing DWI, DCE-MRI, MR elastography, TE, and blood tests [116], MR elastography provided the strongest correlation with fibrosis stage ($r = 0.66$, $P < 0.001$), inflammation grade ($r = 0.52$, $P < 0.001$), and collagen content ($r = 0.53$, $P = 0.036$). For detection of moderate-to-advanced fibrosis (F2–F4), AUCs were 0.78, 0.82, 0.72, 0.79, 0.71 for MR elastography, TE, DCE-MRI, DWI, and APRI, respectively. For detection of advanced fibrosis (F3–F4), AUCs were 0.94, 0.77, 0.79, 0.79, and 0.70, respectively. Overall, DCE-MRI had lower accuracy compared to MR elastography for detecting advanced fibrosis and cirrhosis. Other studies showed that DCE-MRI with gadoteric acid disodium can be used to stage liver fibrosis [146, 147]. In one of these studies, DCE-MRI perfusion was measured with two methods: (1) dual-input single-compartment model for arterial blood flow, portal venous blood flow, total liver blood flow, arterial fraction, distribution volume, and mean transit time; and (2) curve analysis model for peak, slope, and AUC [146]. Slope and AUC were two best perfusion parameters to predict the severity of liver fibrosis ($>$ F2 vs. F2). Four signifi-

cantly different variables were found between nonfibrotic vs. mild-fibrotic subgroups as well: arterial blood flow, arterial fraction, slope, and AUC, and the best predictor for mild fibrosis was arterial blood flow [146]. While this study used a dual-input single-compartment model, a dual-inlet two-compartment uptake model can measure arterial and venous perfusion and hepatic function in a single acquisition [148].

Another study showed that the combination of DCE-MRI (distribution volume and time to peak) and IVIM DWI (ADC) provides an accurate diagnosis of cirrhosis, with 84.6% sensitivity and 100% specificity [120]. Time to peak, distribution volume, and mean transit time were significantly increased in cirrhosis [120].

Quantitative T1, T2, and T1 rho mapping

Quantitative mapping of relaxation parameters has also been explored in the evaluation of liver fibrosis. T1 rho values have been correlated with liver fibrosis in animal models [149]. In chronic liver disease patients, quantitative T1 mapping showed significant changes dependent on Child–Pugh class, with T1 also elevated in stiffer livers (as measured with transient elastography) [150]. Quantitative T2 values have also been shown to increase in patients with hepatitis C, correlating with increasing fibrosis grade [151]. Currently there are no known studies directly comparing these mapping techniques and established elastography techniques. These techniques may prove to have specific applications in hepatic fibrosis.

CT including perfusion, fractional extracellular space, and dual energy

Contrast-enhanced CT methods have been used to assess for the severity of diffuse liver disease and cirrhosis. CT perfusion which involves repeated imaging of the liver after injection of a bolus of IV contrast allows for measurements of increased arterial flow and arterial fractional flow, which correlates moderately with portal hypertension and extent of liver fibrosis [152–154]. With hepatic fibrogenesis, microcirculatory changes result in increased total hepatic resistance with altered portal venous blood flow, compensated by increased hepatic arterial flow (a hepatic artery buffer response) [155, 156]. Arterial perfusion increases with cirrhosis and correlates with severity [154]. Mean arterial enhancement fraction is higher in patients with liver disease compared with those without liver disease. Receiver operating characteristic curve analysis in one study determined an area under the curve of 0.79/0.78, with an optimal cutoff for mean arterial enhancement fraction of 9.2/16.8, for differentiating between category 2 or higher/category 3 disease [152].

Perfusion changes occurring early during fibrosis in chronic hepatitis C can be detected with perfusion CT [153], and may help to discriminate minimal from intermediate stage fibrosis. Mean transit time was the most promising perfusion parameter for differentiating between fibrosis stages, as a threshold of 13.4 s allowed discrimination between minimal and intermediate fibrosis with 71% sensitivity and 65% specificity [153]. However, the authors cautioned against using this parameter for individual patients due to the large overlap between fibrosis groups. Though promising, CT perfusion techniques require higher radiation dose than a routine CT and significant post-processing.

More recently, CT techniques that require less radiation dose and simpler processing have been studied. Fractional extracellular space (also termed equilibrium phase imaging) with or without dual-energy or spectral CT assesses for expansion of the extracellular space, such as occurs by the deposition of collagen fibers in liver fibrosis. Fractional extracellular space (fECS) requires an unenhanced CT scan and a delayed/equilibrium phase scan (at least 5 min scan delay), and is calculated as the enhancement of the (Liver/Aorta) * (1 - Hct) during the equilibrium phase [157]. A retrospective study showed that noninvasive contrast-enhanced CT quantification of the fractional extracellular space correlates with the MELD score, an indicator of the severity of liver disease [158]. Subjectively, the fractional extracellular space in fibrotic liver is expanded, creating an increased volume of distribution within the parenchyma for extracellular contrast and may show similar enhancement to vasculature at equilibrium phase. During the equilibrium phase a large amount of contrast diffuses into the liver leading to abnormally high attenuation. Normal liver is darker than vasculature at equilibrium phase because the fractional extracellular space is low in the parenchyma. While conventional CT perfusion is fair at predicting cirrhosis/portal hypertension (AUC = 0.732), fractional extracellular space is excellent at predicting cirrhosis with an AUC of 0.953 ($P < 0.0001$) [158]. An expanded fractional extracellular space greater than 30% for the prediction of cirrhosis had 92% sensitivity and 83% specificity [158]. A recent study showed comparing fECS on MRI with MR elastography showed modest correlation of fECS with liver stiffness. In this study, fECS at 10 min post intravenous gadolinium injection had a sensitivity of 67%, specificity of 66% and accuracy of 72% for detecting advanced fibrosis as determined by MRE [159]. Although excellent differentiation of cirrhosis from early-stage fibrosis was seen with extracellular space measurements, more modest results were seen for predicting the stage of liver fibrosis [160–162].

Dual-energy CT can estimate the fractional extracellular space with a single equilibrium (delayed) phase CT scan since the iodine concentration can be calculated without the need for an additional unenhanced CT scan.

It utilizes high and low x-ray energy datasets to generate qualitative and quantitative material-specific (“material density”) imaging information [163]. As research suggests a correlation between iodine concentrations on delayed phase images with higher stages of fibrosis [164], a normalized iodine concentration (liver/aorta) can be used to estimate the degree of disease. In a study using dual-energy or spectral CT, the combination of normalized iodine concentration and iodine concentration ratio showed high sensitivity and specificity for differentiating healthy liver from cirrhotic liver, especially in Class C cirrhotic liver [165]. Another study on spectral CT showed that the arterial iodine fraction was statistically significantly different between a control group and patients with chronic liver disease Child–Pugh Grades A, B, and C [166].

Contrast-enhanced ultrasound

Contrast-enhanced ultrasound (CE US) of the liver is mainly used to characterize focal liver lesions [167], although research has studied the use of contrast-enhanced US in diagnosing fibrosis and cirrhosis. US contrast has recently been approved for liver applications in the United States. Some studies show that CE US can exclude cirrhosis using contrast agent transit or disappearance times, but is not effective for staging fibrosis [51, 168, 169].

Shortening of the transit time between the hepatic artery/portal vein and the hepatic veins occurs in both cirrhosis and liver malignancies, presumably because of intrahepatic shunting, which limits its usefulness in the diagnosis of fibrosis [167, 170, 171]. One study showed that quantitative measurements of intrahepatic transit time were significantly correlated with the severity of liver fibrosis. The hepatic artery to hepatic vein transit time and portal vein to hepatic vein transit time were shortened gradually with the progression of liver fibrosis [170].

Another study showed that hepatic vein transit time in CE US of hepatitis C patients can differentiate between mild hepatitis and cirrhosis, with 100% sensitivity and 80% specificity for diagnosing cirrhosis and 95% sensitivity and 86% specificity for differentiating mild hepatitis from more severe liver disease [171]. However, another study showed poor sensitivity (57%) and specificity (43%) using hepatic vein transit time as a marker for hepatic fibrosis [172].

Texture analysis

Texture analysis is a new and expanding area of imaging research, and may have a role in assessing liver fibrosis. Texture analysis is a type of computer-aided image analysis whereby mathematical transformations and statistical analysis are applied to the distribution of grayscale values in an image [173]. This permits quan-

tification of “texture features” that can then be correlated with disease. In studying liver fibrosis, texture analysis of the liver parenchyma has been applied to US [174, 175], MRI including DWI [173], unenhanced T2 [176, 177], proton density [178], double contrast-enhanced [179, 180], and hepatobiliary-enhanced [181] sequences, and CT [182–184]. Texture analysis is a broad and heterogeneous field, with considerable variability in the texture features that are considered, methods of measurement, and strategies for quantification. This variability makes it difficult to compare studies, and further standardization will eventually be required. Larger studies and studies comparing them with other techniques for evaluation of hepatic fibrosis are awaited.

Direct molecular imaging probes of collagen

The tools currently used to noninvasively detect liver fibrosis described throughout this review are all indirect measures of the pathologic process (inflammation and fibrosis). Several noninvasive imaging techniques are under development to directly detect the deposition of collagen, which may be especially helpful in detecting mild disease. To date, all studies have been in animal models. For example, a gadolinium-based probe, EP-3533, has been explored in two different rodent models of liver fibrosis [185, 186]. Recent studies suggest that EP-3533 may be synergistic with MR elastography, with changes in EP-3533 signal dominant in early fibrosis and MR elastography changes dominant in late fibrosis [187]. An alternative molecular imaging approach has been to develop molecular markers that specifically target hepatic stellate cells [188, 189]. These molecular approaches are attractive because they aim to directly image the pathological changes underlying liver fibrosis. However, considerable development is still required prior to clinical translation.

Future research needs

Research will continue to improve noninvasive diagnosis and staging of liver fibrosis with conventional and novel techniques. Future research needs in the fields of US elastography and MR elastography of the liver involve monitoring hepatic fibrosis after treatment, prognostication of hepatic complications including decompensation of cirrhosis and development of HCC, subclassification of patients with cirrhosis, detection of inflammation, since fibrosis and inflammation can both contribute to increased liver stiffness, and predicting portal hypertension, including spleen stiffness [64, 190]. Technical areas of research interest in US and MR elastography include 3D measurement of tissue displacement, multifrequency elastography, standardization of terminology, calibration of elastography measurements, and harmonization of the different elastography

techniques [64]. Further research is also needed to assess if and how the results of these various imaging methods of diagnosing and staging liver fibrosis are affected by the various etiologies of chronic liver disease, such as hepatitis B, hepatitis C, alcoholic liver disease, and NAFLD.

Conclusions

Hepatic fibrosis is potentially reversible; however, early diagnosis is necessary for treatment in order to halt progression to cirrhosis and development of complications including portal hypertension and hepatocellular carcinoma. Morphologic signs of cirrhosis on US, CT, and MRI alone are unreliable and are seen with more advanced disease.

Newer imaging techniques to diagnose liver fibrosis are reliable and accurate, and include MR elastography and US elastography (TE and SWE or ARFI). MR elastography is the most accurate noninvasive method of diagnosing liver fibrosis, as it can assess the whole liver. TE has been heavily researched and validated in diagnosing liver fibrosis. However, TE is unreliable in patients with NAFLD, ascites, and obesity without an XL probe, whereas point SWE or ARFI can be used in these patients and can be easily added to grayscale US.

Research is ongoing with multiple other techniques for the noninvasive diagnosis of liver fibrosis, including MRI with diffusion weighted imaging, hepatobiliary contrast enhancement, and perfusion; CT using perfusion, fractional extracellular space techniques, and dual-energy, contrast-enhanced US, texture analysis in multiple modalities, quantitative mapping, and direct molecular imaging probes. Research on hepatic fibrosis will continue to validate and improve these techniques, and over time they will become more reliable and easier to apply in the clinical setting. Efforts to advance the noninvasive imaging assessment of hepatic fibrosis will facilitate earlier diagnosis and improved patient monitoring with the goal of preventing the progression to cirrhosis and its complications.

Acknowledgments. The authors thank Dr. Michael R. Savino for assistance with images and Dr. Claude Sirlin and Dr. Venkateswar R. Surabhi, other members of the Society of Abdominal Radiology Disease Focus Panel.

Compliance with Ethical Standards

Funding This study is not funded.

Conflict of interest Richard L. Ehman: RLE and the Mayo Clinic have intellectual property rights and a financial interest in MRE technology. RLE serves as CEO and holds equity in Resoundant, Inc. Frank H. Miller MD has received a research grant from Siemens (no financial interest or funds). Michael A. Ohliger has received research support from Gilead pharmaceuticals. Bachir Taouli has received industry research grants from Guerbet and Bayer, is a consultant for Bioclinica, Median Technologies, and has received equipment support from Siemens. The other authors including Jeanne M. Horowitz,

Sudhakar K, Venkatesh, Kartik Jhaveri, Patrick Kamath, Anthony E. Samir, Alvin C. Silva, Michael S. Torbenson, Michael L. Wells, and Benjamin Yeh declare that they have no conflict of interest.

Ethical approval This article does not contain any studies with human participants or animals performed by any of the authors.

References

- Friedman SL (2003) Liver fibrosis—from bench to bedside. *J Hepatol* 38(Suppl 1):S38–S53
- Goodman Z, Becker RJ, Pockros P, Afdhal N (2007) Progression of fibrosis in advanced chronic hepatitis C: evaluation by morphometric image analysis. *Hepatology* 45(4):886–894. doi:10.1002/hep.21595
- Shiffman ML, Stravitz RT, Contos MJ, et al. (2004) Histologic recurrence of chronic hepatitis C virus in patients after living donor and deceased donor liver transplantation. *Liver Transpl* 10(10):1248–1255. doi:10.1002/lt.20232
- Lee YA, Wallace MC, Friedman SL (2015) Pathobiology of liver fibrosis: a translational success story. *Gut* 64(5):830–841. doi:10.1136/gutjnl-2014-306842
- Schuppan D (1990) Structure of the extracellular matrix in normal and fibrotic liver: collagens and glycoproteins. *Semin Liver Dis* 10(1):1–10. doi:10.1055/s-2008-1040452
- Rojkind M, Ponce-Noyola P (1982) The extracellular matrix of the liver. *Coll Relat Res* 2(2):151–175
- Pinzani M, Rombouts K (2004) Liver fibrosis: from the bench to clinical targets. *Dig Liver Dis* 36(4):231–242. doi:10.1016/j.dld.2004.01.003
- Pinzani M, Rombouts K, Colagrande S (2005) Fibrosis in chronic liver diseases: diagnosis and management. *J Hepatol* 42(Suppl 1):S22–36. doi:10.1016/j.jhep.2004.12.008
- Ratziu V, Charlotte F, Heurtier A, et al. (2005) Sampling variability of liver biopsy in nonalcoholic fatty liver disease. *Gastroenterology* 128(7):1898–1906. doi:10.1053/j.gastro.2005.03.084
- Regev A, Berho M, Jeffers LJ, et al. (2002) Sampling error and intraobserver variation in liver biopsy in patients with chronic HCV infection. *Am J Gastroenterol* 97(10):2614–2618. doi:10.1111/j.1572-0241.2002.06038.x
- Chen J, Yin M, Talwalkar JA, et al. (2017) Diagnostic performance of MR elastography and vibration-controlled transient elastography in the detection of hepatic fibrosis in patients with severe to morbid obesity. *Radiology* 283(2):418–428. doi:10.1148/radiol.2016160685
- Dai DF, Swanson PE, Krieger EV, et al. (2014) Congestive hepatic fibrosis score: a novel histologic assessment of clinical severity. *Mod Pathol* 27(12):1552–1558. doi:10.1038/modpathol.2014.79
- Brunt EM, Janney CG, Di Bisceglie AM, Neuschwander-Tetri BA, Bacon BR (1999) Nonalcoholic steatohepatitis: a proposal for grading and staging the histological lesions. *Am J Gastroenterol* 94(9):2467–2474. doi:10.1111/j.1572-0241.1999.01377.x
- Standish RA, Cholongitas E, Dhillon A, Burroughs AK, Dhillon AP (2006) An appraisal of the histopathological assessment of liver fibrosis. *Gut* 55(4):569–578. doi:10.1136/gut.2005.084475
- Biagini G, Ballardini G (1989) Liver fibrosis and extracellular matrix. *J Hepatol* 8(1):115–124
- Lazzarini AL, Levine RA, Ploutz-Snyder RJ, Sanderson SO (2005) Advances in digital quantification technique enhance discrimination between mild and advanced liver fibrosis in chronic hepatitis C. *Liver Int* 25(6):1142–1149. doi:10.1111/j.1478-3231.2005.01155.x
- Knodell RG, Ishak KG, Black WC, et al. (1981) Formulation and application of a numerical scoring system for assessing histological activity in asymptomatic chronic active hepatitis. *Hepatology* 1(5):431–435
- Bedossa P, Poynard T (1996) An algorithm for the grading of activity in chronic hepatitis C. The METAVIR Cooperative Study Group. *Hepatology* 24(2):289–293. doi:10.1002/hep.510240201
- Batts KP, Ludwig J (1995) Chronic hepatitis. An update on terminology and reporting. *Am J Surg Pathol* 19(12):1409–1417
- Elphick DA, Dube AK, McFarlane E, Jones J, Gleeson D (2007) Spectrum of liver histology in presumed decompensated alcoholic liver disease. *Am J Gastroenterol* 102(4):780–788. doi:10.1111/j.1572-0241.2006.01034.x
- Kakuda Y, Harada K, Sawada-Kitamura S, et al. (2013) Evaluation of a new histologic staging and grading system for primary biliary cirrhosis in comparison with classical systems. *Hum Pathol* 44(6):1107–1117. doi:10.1016/j.humpath.2012.09.017
- Portmann B, Zen Y (2012) Inflammatory disease of the bile ducts—cholangiopathies: liver biopsy challenge and clinicopathological correlation. *Histopathology* 60(2):236–248. doi:10.1111/j.1365-2559.2011.03853.x
- Kim MY, Cho MY, Baik SK, et al. (2011) Histological subclassification of cirrhosis using the Laennec fibrosis scoring system correlates with clinical stage and grade of portal hypertension. *J Hepatol* 55(5):1004–1009. doi:10.1016/j.jhep.2011.02.012
- Rastogi A, Maiwall R, Bihari C, et al. (2013) Cirrhosis histology and Laennec staging system correlate with high portal pressure. *Histopathology* 62(5):731–741. doi:10.1111/his.12070
- Nagula S, Jain D, Groszmann RJ, Garcia-Tsao G (2006) Histological-hemodynamic correlation in cirrhosis—a histological classification of the severity of cirrhosis. *J Hepatol* 44(1):111–117. doi:10.1016/j.jhep.2005.07.036
- Tsochatzis E, Bruno S, Isgro G, et al. (2014) Collagen proportionate area is superior to other histological methods for subclassifying cirrhosis and determining prognosis. *J Hepatol* 60(5):948–954. doi:10.1016/j.jhep.2013.12.023
- Kumar M, Sakhuja P, Kumar A, et al. (2008) Histological subclassification of cirrhosis based on histological-haemodynamic correlation. *Aliment Pharmacol Ther* 27(9):771–779. doi:10.1111/j.1365-2036.2008.03653.x
- Guido M (2011) Chronic hepatitis: grading and staging. In: Saxena R (ed). *Practical Hepatic Pathology: A Diagnostic Approach*. St. Louis: WB Saunders, pp 201–213. doi:10.1016/B978-0-443-06803-4.00016-2
- Goodman ZD, Stoddard AM, Bonkovsky HL, et al. (2009) Fibrosis progression in chronic hepatitis C: morphometric image analysis in the HALT-C trial. *Hepatology* 50(6):1738–1749. doi:10.1002/hep.23211
- Chou R, Wasson N (2013) Blood tests to diagnose fibrosis or cirrhosis in patients with chronic hepatitis C virus infection: a systematic review. *Ann Intern Med* 158(11):807–820. doi:10.7326/0003-4819-158-11-201306040-00005
- Parkes J, Guha IN, Roderick P, Rosenberg W (2006) Performance of serum marker panels for liver fibrosis in chronic hepatitis C. *J Hepatol* 44(3):462–474. doi:10.1016/j.jhep.2005.10.019
- Udell JA, Wang CS, Timmouth J, et al. (2012) Does this patient with liver disease have cirrhosis? *Jama* 307(8):832–842. doi:10.1001/jama.2012.186
- Tan KC (2008) Enlargement of the hilar periportal space. *Radiology* 248(2):699–700. doi:10.1148/radiol.2482060463
- Ito K, Mitchell DG, Gabata T (2000) Enlargement of hilar periportal space: a sign of early cirrhosis at MR imaging. *J Magn Reson Imaging* 11(2):136–140
- Awaya H, Mitchell DG, Kamishima T, et al. (2002) Cirrhosis: modified caudate-right lobe ratio. *Radiology* 224(3):769–774. doi:10.1148/radiol.2243011495
- Di Lelio A, Cestari C, Lomazzi A, Beretta L (1989) Cirrhosis: diagnosis with sonographic study of the liver surface. *Radiology* 172(2):389–392
- Giorgio A, Amoroso P, Lettieri G, et al. (1986) Cirrhosis: value of caudate to right lobe ratio in diagnosis with US. *Radiology* 161(2):443–445. doi:10.1148/radiology.161.2.3532188
- Ito K, Mitchell DG, Gabata T, Hussain SM (1999) Expanded gallbladder fossa: simple MR imaging sign of cirrhosis. *Radiology* 211(3):723–726. doi:10.1148/radiology.211.3.r99ma31723
- Ito K, Mitchell DG, Kim MJ, et al. (2003) Right posterior hepatic notch sign: a simple diagnostic MR finding of cirrhosis. *J Magn Reson Imaging* 18(5):561–566. doi:10.1002/jmri.10387
- Lafortune M, Matricardi L, Denys A, et al. (1998) Segment 4 (the quadrate lobe): a barometer of cirrhotic liver disease at US. *Radiology* 206(1):157–160. doi:10.1148/radiology.206.1.9423666
- Simonovsky V (1999) The diagnosis of cirrhosis by high resolution ultrasound of the liver surface. *Br J Radiol* 72(853):29–34
- Tan KC (2008) The right posterior hepatic notch sign. *Radiology* 248(1):317–318. doi:10.1148/radiol.2481051024

43. Torres WE, Whitmire LF, Gedgaudas-McClees K, Bernardino ME (1986) Computed tomography of hepatic morphologic changes in cirrhosis of the liver. *J Comput Assist Tomogr* 10(1):47–50
44. Yu JS, Shim JH, Chung JJ, Kim JH, Kim KW (2010) Double contrast-enhanced MRI of viral hepatitis-induced cirrhosis: correlation of gross morphological signs with hepatic fibrosis. *Br J Radiol* 83(987):212–217. doi:10.1259/bjr/70974553
45. Zhang Y, Zhang XM, Prowda JC, et al. (2009) Changes in hepatic venous morphology with cirrhosis on MRI. *J Magn Reson Imaging* 29(5):1085–1092. doi:10.1002/jmri.21718
46. Rustogi R, Horowitz J, Harmath C, et al. (2012) Accuracy of MR elastography and anatomic MR imaging features in the diagnosis of severe hepatic fibrosis and cirrhosis. *J Magn Reson Imaging* 35(6):1356–1364. doi:10.1002/jmri.23585
47. Venkatesh SK, Yin M, Takahashi N, et al. (2015) Non-invasive detection of liver fibrosis: MR imaging features vs. MR elastography. *Abdom Imaging* 40(4):766–775. doi:10.1007/s00261-015-0347-6
48. Aube C, Oberti F, Korali N, et al. (1999) Ultrasonographic diagnosis of hepatic fibrosis or cirrhosis. *J Hepatol* 30(3):472–478
49. Allan R, Thoirs K, Phillips M (2010) Accuracy of ultrasound to identify chronic liver disease. *World J Gastroenterol* 16(28):3510–3520
50. Colli A, Colucci A, Paggi S, et al. (2005) Accuracy of a predictive model for severe hepatic fibrosis or cirrhosis in chronic hepatitis C. *World J Gastroenterol* 11(46):7318–7322
51. Bonekamp S, Kamel I, Solga S, Clark J (2009) Can imaging modalities diagnose and stage hepatic fibrosis and cirrhosis accurately? *J Hepatol* 50(1):17–35. doi:10.1016/j.jhep.2008.10.016
52. Tchelepi H, Ralls PW, Radin R, Grant E (2002) Sonography of diffuse liver disease. *J Ultrasound Med* 21(9):1023–1032 (quiz 1033–1024)
53. Hultcrantz R, Gabrielsson N (1993) Patients with persistent elevation of aminotransferases: investigation with ultrasonography, radionuclide imaging and liver biopsy. *J Intern Med* 233(1):7–12
54. Mathiesen UL, Franzen LE, Aselius H, et al. (2002) Increased liver echogenicity at ultrasound examination reflects degree of steatosis but not of fibrosis in asymptomatic patients with mild/moderate abnormalities of liver transaminases. *Dig Liver Dis* 34(7):516–522
55. Haktanir A, Cihan BS, Celenk C, Cihan S (2005) Value of Doppler sonography in assessing the progression of chronic viral hepatitis and in the diagnosis and grading of cirrhosis. *J Ultrasound Med* 24(3):311–321
56. Kawanaka H, Kinjo N, Anegawa G, et al. (2008) Abnormality of the hepatic vein waveforms in cirrhotic patients with portal hypertension and its prognostic implications. *J Gastroenterol Hepatol* 23(7 Pt 2):e129–e136. doi:10.1111/j.1440-1746.2007.05155.x
57. Oguzkurt L, Yildirim T, Torun D, et al. (2005) Hepatic vein Doppler waveform in patients with diffuse fatty infiltration of the liver. *Eur J Radiol* 54(2):253–257. doi:10.1016/j.ejrad.2004.05.011
58. Bernatik T, Strobel D, Hahn EG, Becker D (2002) Doppler measurements: a surrogate marker of liver fibrosis? *Eur J Gastroenterol Hepatol* 14(4):383–387
59. Tang A, Cloutier G, Szevenenyi NM, Sirlin CB (2015) Ultrasound elastography and MR elastography for assessing liver fibrosis: part 1, principles and techniques. *Am J Roentgenol* 205(1):22–32. doi:10.2214/AJR.15.14552
60. Bota S, Herkner H, Sporea I, et al. (2013) Meta-analysis: ARFI elastography versus transient elastography for the evaluation of liver fibrosis. *Liver Int* 33(8):1138–1147. doi:10.1111/liv.12240
61. Friedrich-Rust M, Ong MF, Martens S, et al. (2008) Performance of transient elastography for the staging of liver fibrosis: a meta-analysis. *Gastroenterology* 134(4):960–974. doi:10.1053/j.gastro.2008.01.034
62. Talwalkar JA, Kurtz DM, Schoenleber SJ, West CP, Montori VM (2007) Ultrasound-based transient elastography for the detection of hepatic fibrosis: systematic review and meta-analysis. *Clin Gastroenterol Hepatol* 5(10):1214–1220. doi:10.1016/j.cgh.2007.07.020
63. Tsochatzis EA, Gurusamy KS, Ntaoula S, et al. (2011) Elastography for the diagnosis of severity of fibrosis in chronic liver disease: a meta-analysis of diagnostic accuracy. *J Hepatol* 54(4):650–659. doi:10.1016/j.jhep.2010.07.033
64. Tang A, Cloutier G, Szevenenyi NM, Sirlin CB (2015) Ultrasound elastography and MR elastography for assessing liver fibrosis: part 2, diagnostic performance, confounders, and future directions. *Am J Roentgenol* 205(1):33–40. doi:10.2214/AJR.15.14553
65. Ferraioli G, Tinelli C, Dal Bello B, et al. (2013) Performance of liver stiffness measurements by transient elastography in chronic hepatitis. *World J Gastroenterol* 19(1):49–56. doi:10.3748/wjg.v19.i1.49
66. Kim SU, Han KH, Ahn SH (2010) Transient elastography in chronic hepatitis B: an Asian perspective. *World J Gastroenterol* 16(41):5173–5180
67. Reiberger T, Ferlitsch A, Payer BA, et al. (2012) Noninvasive screening for liver fibrosis and portal hypertension by transient elastography—a large single center experience. *Wien Klin Wochenschr* 124(11–12):395–402. doi:10.1007/s00508-012-0190-5
68. Degos F, Perez P, Roche B, et al. (2010) Diagnostic accuracy of FibroScan and comparison to liver fibrosis biomarkers in chronic viral hepatitis: a multicenter prospective study (the FIBROSTIC study). *J Hepatol* 53(6):1013–1021. doi:10.1016/j.jhep.2010.05.035
69. Myers RP, Pomier-Layrargues G, Kirsch R, et al. (2012) Discordance in fibrosis staging between liver biopsy and transient elastography using the FibroScan XL probe. *J Hepatol* 56(3):564–570. doi:10.1016/j.jhep.2011.10.007
70. Friedrich-Rust M, Hadji-Hosseini H, Kriener S, et al. (2010) Transient elastography with a new probe for obese patients for non-invasive staging of non-alcoholic steatohepatitis. *Eur Radiol* 20(10):2390–2396. doi:10.1007/s00330-010-1820-9
71. Naveau S, Lamouri K, Pourcher G, et al. (2014) The diagnostic accuracy of transient elastography for the diagnosis of liver fibrosis in bariatric surgery candidates with suspected NAFLD. *Obes Surg* 24(10):1693–1701. doi:10.1007/s11695-014-1235-9
72. Yoneda M, Suzuki K, Kato S, et al. (2010) Nonalcoholic fatty liver disease: US-based acoustic radiation force impulse elastography. *Radiology* 256(2):640–647. doi:10.1148/radiol.10091662
73. Palmeri ML, Wang MH, Rouze NC, et al. (2011) Noninvasive evaluation of hepatic fibrosis using acoustic radiation force-based shear stiffness in patients with nonalcoholic fatty liver disease. *J Hepatol* 55(3):666–672. doi:10.1016/j.jhep.2010.12.019
74. Ochi H, Hirooka M, Koizumi Y, et al. (2012) Real-time tissue elastography for evaluation of hepatic fibrosis and portal hypertension in nonalcoholic fatty liver diseases. *Hepatology* 56(4):1271–1278. doi:10.1002/hep.25756
75. Friedrich-Rust M, Romen D, Vermehren J, et al. (2012) Acoustic radiation force impulse-imaging and transient elastography for non-invasive assessment of liver fibrosis and steatosis in NAFLD. *Eur J Radiol* 81(3):e325–e331. doi:10.1016/j.ejrad.2011.10.029
76. Guzman-Aroca F, Frutos-Bernal MD, Bas A, et al. (2012) Detection of non-alcoholic steatohepatitis in patients with morbid obesity before bariatric surgery: preliminary evaluation with acoustic radiation force impulse imaging. *Eur Radiol* 22(11):2525–2532. doi:10.1007/s00330-012-2505-3
77. Sirlin R, Bota S, Sporea I, et al. (2013) Liver stiffness measurements by means of supersonic shear imaging in patients without known liver pathology. *Ultrasound Med Biol* 39(8):1362–1367. doi:10.1016/j.ultrasmedbio.2013.03.021
78. Sporea I, Bota S, Gradinaru-Tascau O, et al. (2014) Which are the cut-off values of 2D-shear wave elastography (2D-SWE) liver stiffness measurements predicting different stages of liver fibrosis, considering transient elastography (TE) as the reference method? *Eur J Radiol* 83(3):e118–e122. doi:10.1016/j.ejrad.2013.12.011
79. Muller M, Gennisson JL, Defieux T, Tanter M, Fink M (2009) Quantitative viscoelasticity mapping of human liver using supersonic shear imaging: preliminary in vivo feasibility study. *Ultrasound Med Biol* 35(2):219–229. doi:10.1016/j.ultrasmedbio.2008.08.018
80. Gerber L, Kasper D, Fitting D, et al. (2015) Assessment of liver fibrosis with 2-D shear wave elastography in comparison to transient elastography and acoustic radiation force impulse imaging in patients with chronic liver disease. *Ultrasound Med Biol* 41(9):2350–2359. doi:10.1016/j.ultrasmedbio.2015.04.014
81. Samir AE, Dhyani M, Vij A, et al. (2015) Shear-wave elastography for the estimation of liver fibrosis in chronic liver disease:

- determining accuracy and ideal site for measurement. *Radiology* 274(3):888–896. doi:10.1148/radiol.14140839
82. Sporea I, Sirli RL, Deleanu A, et al. (2011) Acoustic radiation force impulse elastography as compared to transient elastography and liver biopsy in patients with chronic hepatopathies. *Ultraschall Med* 32(Suppl 1):S46–S52. doi:10.1055/s-0029-1245360
 83. Goertz RS, Zopf Y, Jugl V, et al. (2010) Measurement of liver elasticity with acoustic radiation force impulse (ARFI) technology: an alternative noninvasive method for staging liver fibrosis in viral hepatitis. *Ultraschall Med* 31(2):151–155. doi:10.1055/s-0029-1245244
 84. Karlas T, Pfrepper C, Troeltzsch M, Wiegand J, Keim V (2010) Acoustic radiation force impulse liver stiffness measurement: interlobe differences demand standardized examination procedures. *Eur J Gastroenterol Hepatol* 22(11):1387. doi:10.1097/MEG.0b013e32833caf8e
 85. Mederacke I, Wursthorn K, Kirschner J, et al. (2009) Food intake increases liver stiffness in patients with chronic or resolved hepatitis C virus infection. *Liver Int* 29(10):1500–1506. doi:10.1111/j.1478-3231.2009.02100.x
 86. Popescu A, Bota S, Sporea I, et al. (2013) The influence of food intake on liver stiffness values assessed by acoustic radiation force impulse elastography—preliminary results. *Ultrasound Med Biol* 39(4):579–584. doi:10.1016/j.ultrasmedbio.2012.11.013
 87. Arena U, Vizzutti F, Corti G, et al. (2008) Acute viral hepatitis increases liver stiffness values measured by transient elastography. *Hepatology* 47(2):380–384. doi:10.1002/hep.22007
 88. Millonig G, Reimann FM, Friedrich S, et al. (2008) Extrahepatic cholestasis increases liver stiffness (FibroScan) irrespective of fibrosis. *Hepatology* 48(5):1718–1723. doi:10.1002/hep.22577
 89. Millonig G, Friedrich S, Adolf S, et al. (2010) Liver stiffness is directly influenced by central venous pressure. *J Hepatol* 52(2):206–210. doi:10.1016/j.jhep.2009.11.018
 90. Venkatesh SK, Ehman RL (2015) Magnetic resonance elastography of abdomen. *Abdom Imaging* 40(4):745–759. doi:10.1007/s00261-014-0315-6
 91. Venkatesh SK, Yin M, Ehman RL (2013) Magnetic resonance elastography of liver: technique, analysis, and clinical applications. *J Magn Reson Imaging* 37(3):544–555. doi:10.1002/jmri.23731
 92. Singh S, Venkatesh SK, Wang Z, et al. (2015) Diagnostic performance of magnetic resonance elastography in staging liver fibrosis: a systematic review and meta-analysis of individual participant data. *Clin Gastroenterol Hepatol* 13(3):440–451 e446. doi:10.1016/j.cgh.2014.09.046
 93. Guo Y, Parthasarathy S, Goyal P, et al. (2014) Magnetic resonance elastography and acoustic radiation force impulse for staging hepatic fibrosis: a meta-analysis. *Abdom Imaging* . doi:10.1007/s00261-014-0137-6
 94. Godfrey EM, Patterson AJ, Priest AN, et al. (2012) A comparison of MR elastography and 31P MR spectroscopy with histological staging of liver fibrosis. *Eur Radiol* 22(12):2790–2797. doi:10.1007/s00330-012-2527-x
 95. Hines CD, Bley TA, Lindstrom MJ, Reeder SB (2010) Repeatability of magnetic resonance elastography for quantification of hepatic stiffness. *J Magn Reson Imaging* 31(3):725–731. doi:10.1002/jmri.22066
 96. Lee DH, Lee JM, Han JK, Choi BI (2013) MR elastography of healthy liver parenchyma: normal value and reliability of the liver stiffness value measurement. *J Magn Reson Imaging* 38(5):1215–1223. doi:10.1002/jmri.23958
 97. Venkatesh SK, Wang G, Teo LL, Ang BW (2014) Magnetic resonance elastography of liver in healthy Asians: normal liver stiffness quantification and reproducibility assessment. *J Magn Reson Imaging* 39(1):1–8. doi:10.1002/jmri.24084
 98. Wang QB, Zhu H, Liu HL, Zhang B (2012) Performance of magnetic resonance elastography and diffusion-weighted imaging for the staging of hepatic fibrosis: a meta-analysis. *Hepatology* 56(1):239–247. doi:10.1002/hep.25610
 99. Castera L, Foucher J, Bernard PH, et al. (2010) Pitfalls of liver stiffness measurement: a 5-year prospective study of 13,369 examinations. *Hepatology* 51(3):828–835. doi:10.1002/hep.23425
 100. Bota S, Sporea I, Sirli R, et al. (2014) Factors associated with the impossibility to obtain reliable liver stiffness measurements by means of Acoustic Radiation Force Impulse (ARFI) elastography—analysis of a cohort of 1,031 subjects. *Eur J Radiol* 83(2):268–272. doi:10.1016/j.ejrad.2013.11.019
 101. Huwart L, Sempoux C, Vicaux E, et al. (2008) Magnetic resonance elastography for the noninvasive staging of liver fibrosis. *Gastroenterology* 135(1):32–40. doi:10.1053/j.gastro.2008.03.076
 102. Ichikawa S, Motosugi U, Ichikawa T, et al. (2012) Magnetic resonance elastography for staging liver fibrosis in chronic hepatitis C. *MRMS* 11(4):291–297
 103. Kim D, Kim WR, Talwalkar JA, Kim HJ, Ehman RL (2013) Advanced fibrosis in nonalcoholic fatty liver disease: noninvasive assessment with MR elastography. *Radiology* 268(2):411–419. doi:10.1148/radiol.13121193
 104. Venkatesh SK, Wang G, Lim SG, Wee A (2014) Magnetic resonance elastography for the detection and staging of liver fibrosis in chronic hepatitis B. *Eur Radiol* 24(1):70–78. doi:10.1007/s00330-013-2978-8
 105. Yin M, Talwalkar JA, Glaser KJ, et al. (2007) Assessment of hepatic fibrosis with magnetic resonance elastography. *Clin Gastroenterol Hepatol* 5(10):1207–1213.e1202. doi:10.1016/j.cgh.2007.06.012
 106. Wagner M, Corcuera-Solano I, Lo G, et al. (2017) Technical failure of MR elastography examinations of the liver: experience from a large single-center study. *Radiology* . doi:10.1148/radiol.2016160863
 107. Wagner M, Besa C, Bou Ayache J, et al. (2016) Magnetic resonance elastography of the liver: qualitative and quantitative comparison of gradient echo and spin echo echoplanar imaging sequences. *Invest Radiol* 51(9):575–581. doi:10.1097/RLI.0000000000000269
 108. Yin M, Talwalkar JA, Glaser KJ, et al. (2011) Dynamic postprandial hepatic stiffness augmentation assessed with MR elastography in patients with chronic liver disease. *Am J Roentgenol* 197(1):64–70. doi:10.2214/AJR.10.5989
 109. Jajamovich GH, Dyvorne H, Donnerhack C, Taouli B (2014) Quantitative liver MRI combining phase contrast imaging, elastography, and DWI: assessment of reproducibility and postprandial effect at 3.0 T. *PLoS ONE* 9(5):e97355. doi:10.1371/journal.pone.0097355
 110. Taouli B, Koh DM (2010) Diffusion-weighted MR imaging of the liver. *Radiology* 254(1):47–66. doi:10.1148/radiol.09090021
 111. Luciani A, Vignaud A, Cavet M, et al. (2008) Liver cirrhosis: intravoxel incoherent motion MR imaging—pilot study. *Radiology* 249(3):891–899. doi:10.1148/radiol.2493080080
 112. Yamada I, Aung W, Himeno Y, Nakagawa T, Shibuya H (1999) Diffusion coefficients in abdominal organs and hepatic lesions: evaluation with intravoxel incoherent motion echo-planar MR imaging. *Radiology* 210(3):617–623. doi:10.1148/radiology.210.3.r99fe17617
 113. Annet L, Peeters F, Abarca-Quinones J, et al. (2007) Assessment of diffusion-weighted MR imaging in liver fibrosis. *J Magn Reson Imaging* 25(1):122–128. doi:10.1002/jmri.20771
 114. Taouli B, Tolia AJ, Losada M, et al. (2007) Diffusion-weighted MRI for quantification of liver fibrosis: preliminary experience. *Am J Roentgenol* 189(4):799–806. doi:10.2214/AJR.07.2086
 115. Girometti R, Furlan A, Bazzocchi M, et al. (2007) Diffusion-weighted MRI in evaluating liver fibrosis: a feasibility study in cirrhotic patients. *Radiol Med* 112(3):394–408. doi:10.1007/s11547-007-0149-1
 116. Dyvorne HA, Jajamovich GH, Bane O, et al. (2016) Prospective comparison of magnetic resonance imaging to transient elastography and serum markers for liver fibrosis detection. *Liver Int* 36(5):659–666. doi:10.1111/liv.13058
 117. Wang Y, Ganger DR, Levitsky J, et al. (2011) Assessment of chronic hepatitis and fibrosis: comparison of MR elastography and diffusion-weighted imaging. *Am J Roentgenol* 196(3):553–561. doi:10.2214/AJR.10.4580
 118. Chandarana H, Do RK, Mussi TC, et al. (2012) The effect of liver iron deposition on hepatic apparent diffusion coefficient values in cirrhosis. *AJR Am J Roentgenol* 199(4):803–808. doi:10.2214/ajr.11.7541
 119. Dyvorne HA, Galea N, Nevers T, et al. (2013) Diffusion-weighted imaging of the liver with multiple b values: effect of diffusion gradient polarity and breathing acquisition on image quality and

- intravoxel incoherent motion parameters—a pilot study. *Radiology* 266(3):920–929. doi:[10.1148/radiol.12120686](https://doi.org/10.1148/radiol.12120686)
120. Patel J, Sigmund EE, Rusinek H, et al. (2010) Diagnosis of cirrhosis with intravoxel incoherent motion diffusion MRI and dynamic contrast-enhanced MRI alone and in combination: preliminary experience. *J Magn Reson Imaging* 31(3):589–600. doi:[10.1002/jmri.22081](https://doi.org/10.1002/jmri.22081)
 121. Zhang B, Liang L, Dong Y, et al. (2016) Intravoxel incoherent motion MR imaging for staging of hepatic fibrosis. *PLoS ONE* 11(1):e0147789. doi:[10.1371/journal.pone.0147789](https://doi.org/10.1371/journal.pone.0147789)
 122. Chung SR, Lee SS, Kim N, et al. (2015) Intravoxel incoherent motion MRI for liver fibrosis assessment: a pilot study. *Acta Radiol* 56(12):1428–1436. doi:[10.1177/0284185114559763](https://doi.org/10.1177/0284185114559763)
 123. Ichikawa S, Motosugi U, Morisaka H, et al. (2015) MRI-based staging of hepatic fibrosis: comparison of intravoxel incoherent motion diffusion-weighted imaging with magnetic resonance elastography. *J Magn Reson Imaging* 42(1):204–210. doi:[10.1002/jmri.24760](https://doi.org/10.1002/jmri.24760)
 124. Parente DB, Paiva FF, Oliveira Neto JA, et al. (2015) Intravoxel incoherent motion diffusion weighted MR imaging at 3.0 T: assessment of steatohepatitis and fibrosis compared with liver biopsy in type 2 diabetic patients. *PLoS ONE* 10(5):e0125653. doi:[10.1371/journal.pone.0125653](https://doi.org/10.1371/journal.pone.0125653)
 125. Wu CH, Ho MC, Jeng YM, et al. (2015) Assessing hepatic fibrosis: comparing the intravoxel incoherent motion in MRI with acoustic radiation force impulse imaging in US. *Eur Radiol* 25(12):3552–3559. doi:[10.1007/s00330-015-3774-4](https://doi.org/10.1007/s00330-015-3774-4)
 126. Jhaveri K, Cleary S, Audet P, et al. (2015) Consensus statements from a multidisciplinary expert panel on the utilization and application of a liver-specific MRI contrast agent (gadoteric acid). *Am J Roentgenol* 204(3):498–509. doi:[10.2214/ajr.13.12399](https://doi.org/10.2214/ajr.13.12399)
 127. Ringe KI, Husarik DB, Sirlin CB, Merkle EM (2010) Gadoteric acid-enhanced MRI of the liver: part 1, protocol optimization and lesion appearance in the noncirrhotic liver. *Am J Roentgenol* 195(1):13–28. doi:[10.2214/ajr.10.4392](https://doi.org/10.2214/ajr.10.4392)
 128. Tsuda N, Okada M, Murakami T (2010) New proposal for the staging of nonalcoholic steatohepatitis: evaluation of liver fibrosis on Gd-EOB-DTPA-enhanced MRI. *Eur J Radiol* 73(1):137–142. doi:[10.1016/j.ejrad.2008.09.036](https://doi.org/10.1016/j.ejrad.2008.09.036)
 129. Motosugi U, Ichikawa T, Oguri M, et al. (2011) Staging liver fibrosis by using liver-enhancement ratio of gadoteric acid-enhanced MR imaging: comparison with aspartate aminotransferase-to-platelet ratio index. *Magn Reson Imaging* 29(8):1047–1052. doi:[10.1016/j.mri.2011.05.007](https://doi.org/10.1016/j.mri.2011.05.007)
 130. Watanabe H, Kanematsu M, Goshima S, et al. (2011) Staging hepatic fibrosis: comparison of gadoteric acid-enhanced and diffusion-weighted MR imaging—preliminary observations. *Radiology* 259(1):142–150. doi:[10.1148/radiol.10100621](https://doi.org/10.1148/radiol.10100621)
 131. Hope TA, Doherty A, Fu Y, et al. (2012) Gadolinium accumulation and fibrosis in the liver after administration of gadoteric acid in a rat model of active hepatic fibrosis. *Radiology* 264(2):423–427. doi:[10.1148/radiol.12112453](https://doi.org/10.1148/radiol.12112453)
 132. Goshima S, Kanematsu M, Watanabe H, et al. (2012) Gd-EOB-DTPA-enhanced MR imaging: prediction of hepatic fibrosis stages using liver contrast enhancement index and liver-to-spleen volumetric ratio. *J Magn Reson Imaging* 36(5):1148–1153. doi:[10.1002/jmri.23758](https://doi.org/10.1002/jmri.23758)
 133. Ding Y, Rao S, Yang L, Chen C, Zeng M (2016) Comparison of the effect of region-of-interest methods using gadoteric acid-enhanced MR imaging with diffusion-weighted imaging on staging hepatic fibrosis. *Radiol Med* 121(11):821–827. doi:[10.1007/s11547-016-0669-7](https://doi.org/10.1007/s11547-016-0669-7)
 134. Ding Y, Rao SX, Zhu T, et al. (2015) Liver fibrosis staging using T1 mapping on gadoteric acid-enhanced MRI compared with DW imaging. *Clin Radiol* 70(10):1096–1103. doi:[10.1016/j.crad.2015.04.014](https://doi.org/10.1016/j.crad.2015.04.014)
 135. Park HS, Kim YJ, Yu MH, et al. (2014) Three-Tesla magnetic resonance elastography for hepatic fibrosis: comparison with diffusion-weighted imaging and gadoteric acid-enhanced magnetic resonance imaging. *World J Gastroenterol* 20(46):17558–17567. doi:[10.3748/wjg.v20.i46.17558](https://doi.org/10.3748/wjg.v20.i46.17558)
 136. Kim H, Park SH, Kim EK, et al. (2014) Histogram analysis of gadoteric acid-enhanced MRI for quantitative hepatic fibrosis measurement. *PLoS ONE* 9(12):e114224. doi:[10.1371/journal.pone.0114224](https://doi.org/10.1371/journal.pone.0114224)
 137. Okada M, Murakami T, Yada N, et al. (2015) Comparison between T1 relaxation time of Gd-EOB-DTPA-enhanced MRI and liver stiffness measurement of ultrasound elastography in the evaluation of cirrhotic liver. *J Magn Reson Imaging* 41(2):329–338. doi:[10.1002/jmri.24529](https://doi.org/10.1002/jmri.24529)
 138. Choi YR, Lee JM, Yoon JH, Han JK, Choi BI (2013) Comparison of magnetic resonance elastography and gadoteric acid-enhanced magnetic resonance imaging for the evaluation of hepatic fibrosis. *Invest Radiol* 48(8):607–613. doi:[10.1097/RLI.0b013e318289ff8f](https://doi.org/10.1097/RLI.0b013e318289ff8f)
 139. Noren B, Forsgren MF, Dahlqvist Leinhard O, et al. (2013) Separation of advanced from mild hepatic fibrosis by quantification of the hepatobiliary uptake of Gd-EOB-DTPA. *Eur Radiol* 23(1):174–181. doi:[10.1007/s00330-012-2583-2](https://doi.org/10.1007/s00330-012-2583-2)
 140. Besa C, Bane O, Jajamovich G, Marchione J, Taouli B (2015) 3D T1 relaxometry pre and post gadoteric acid injection for the assessment of liver cirrhosis and liver function. *Magn Reson Imaging* 33(9):1075–1082. doi:[10.1016/j.mri.2015.06.013](https://doi.org/10.1016/j.mri.2015.06.013)
 141. Nassif A, Jia J, Keiser M, et al. (2012) Visualization of hepatic uptake transporter function in healthy subjects by using gadoteric acid-enhanced MR imaging. *Radiology* 264(3):741–750. doi:[10.1148/radiol.12112061](https://doi.org/10.1148/radiol.12112061)
 142. Feier D, Balassy C, Bastati N, et al. (2016) The diagnostic efficacy of quantitative liver MR imaging with diffusion-weighted, SWI, and hepato-specific contrast-enhanced sequences in staging liver fibrosis—a multiparametric approach. *Eur Radiol* 26(2):539–546. doi:[10.1007/s00330-015-3830-0](https://doi.org/10.1007/s00330-015-3830-0)
 143. Sheng RF, Wang HQ, Yang L, et al. (2017) Assessment of liver fibrosis using T1 mapping on Gd-EOB-DTPA-enhanced magnetic resonance. *Dig Liver Dis*. doi:[10.1016/j.dld.2017.02.006](https://doi.org/10.1016/j.dld.2017.02.006)
 144. Yang L, Ding Y, Rao S, et al. (2017) Staging liver fibrosis in chronic hepatitis B with T1 relaxation time index on gadoteric acid-enhanced MRI: comparison with aspartate aminotransferase-to-platelet ratio index and FIB-4. *J Magn Reson Imaging* 45(4):1186–1194. doi:[10.1002/jmri.25440](https://doi.org/10.1002/jmri.25440)
 145. Hagiwara M, Rusinek H, Lee VS, et al. (2008) Advanced liver fibrosis: diagnosis with 3D whole-liver perfusion MR imaging—initial experience. *Radiology* 246(3):926–934. doi:[10.1148/radiol.2463070077](https://doi.org/10.1148/radiol.2463070077)
 146. Chen BB, Hsu CY, Yu CW, et al. (2012) Dynamic contrast-enhanced magnetic resonance imaging with Gd-EOB-DTPA for the evaluation of liver fibrosis in chronic hepatitis patients. *Eur Radiol* 22(1):171–180. doi:[10.1007/s00330-011-2249-5](https://doi.org/10.1007/s00330-011-2249-5)
 147. Xie S, Sun Y, Wang L, et al. (2015) Assessment of liver function and liver fibrosis with dynamic Gd-EOB-DTPA-enhanced MRI. *Acad Radiol* 22(4):460–466. doi:[10.1016/j.acra.2014.11.006](https://doi.org/10.1016/j.acra.2014.11.006)
 148. Sourbron S, Sommer WH, Reiser MF, Zech CJ (2012) Combined quantification of liver perfusion and function with dynamic gadoteric acid-enhanced MR imaging. *Radiology* 263(3):874–883. doi:[10.1148/radiol.12110337](https://doi.org/10.1148/radiol.12110337)
 149. Zhang H, Yang Q, Yu T, et al. (2017) Comparison of T2, T1rho, and diffusion metrics in assessment of liver fibrosis in rats. *J Magn Reson Imaging* 45(3):741–750. doi:[10.1002/jmri.25424](https://doi.org/10.1002/jmri.25424)
 150. Cassinotto C, Feldis M, Vergniol J, et al. (2015) MR relaxometry in chronic liver diseases: comparison of T1 mapping, T2 mapping, and diffusion-weighted imaging for assessing cirrhosis diagnosis and severity. *Eur J Radiol* 84(8):1459–1465. doi:[10.1016/j.ejrad.2015.05.019](https://doi.org/10.1016/j.ejrad.2015.05.019)
 151. Guimaraes AR, Siqueira L, Uppal R, et al. (2016) T2 relaxation time is related to liver fibrosis severity. *Quant Imaging Med Surg* 6(2):103–114. doi:[10.21037/qims.2016.03.02](https://doi.org/10.21037/qims.2016.03.02)
 152. Bonekamp D, Bonekamp S, Geiger B, Kamel IR (2012) An elevated arterial enhancement fraction is associated with clinical and imaging indices of liver fibrosis and cirrhosis. *J Comput Assist Tomogr* 36(6):681–689. doi:[10.1097/RCT.0b013e3182702ee3](https://doi.org/10.1097/RCT.0b013e3182702ee3)
 153. Ronot M, Asselah T, Paradis V, et al. (2010) Liver fibrosis in chronic hepatitis C virus infection: differentiating minimal from intermediate fibrosis with perfusion CT. *Radiology* 256(1):135–142. doi:[10.1148/radiol.10091295](https://doi.org/10.1148/radiol.10091295)
 154. Van Beers BE, Leconte I, Materne R, et al. (2001) Hepatic perfusion parameters in chronic liver disease: dynamic CT measure-

- ments correlated with disease severity. *Am J Roentgenol* 176(3):667–673. doi:10.2214/ajr.176.3.1760667
155. Richter S, Mucke I, Menger MD, Vollmar B (2000) Impact of intrinsic blood flow regulation in cirrhosis: maintenance of hepatic arterial buffer response. *Am J Physiol Gastrointest Liver Physiol* 279(2):G454–G462
 156. Gulberg V, Haag K, Rossle M, Gerbes AL (2002) Hepatic arterial buffer response in patients with advanced cirrhosis. *Hepatology* 35(3):630–634. doi:10.1053/jhep.2002.31722
 157. Varenika V, Fu Y, Maher JJ, et al. (2013) Hepatic fibrosis: evaluation with semiquantitative contrast-enhanced CT. *Radiology* 266(1):151–158. doi:10.1148/radiol.12112452
 158. Zissen MH, Wang ZJ, Yee J, et al. (2013) Contrast-enhanced CT quantification of the hepatic fractional extracellular space: correlation with diffuse liver disease severity. *Am J Roentgenol* 201(6):1204–1210. doi:10.2214/AJR.12.10039
 159. Wells ML, Moynagh MR, Carter RE, et al. (2017) Correlation of hepatic fractional extracellular space using gadolinium enhanced MRI with liver stiffness using magnetic resonance elastography. *Abdom Radiol (NY)* 42(1):191–198. doi:10.1007/s00261-016-0867-8
 160. Yoon JH, Lee JM, Klotz E, et al. (2015) Estimation of hepatic extracellular volume fraction using multiphasic liver computed tomography for hepatic fibrosis grading. *Invest Radiol* 50(4):290–296. doi:10.1097/rli.000000000000123
 161. Bandula S, Punwani S, Rosenberg WM, et al. (2015) Equilibrium contrast-enhanced CT imaging to evaluate hepatic fibrosis: initial validation by comparison with histopathologic sampling. *Radiology* 275(1):136–143. doi:10.1148/radiol.14141435
 162. Guo SL, Su LN, Zhai YN, et al. (2017) The clinical value of hepatic extracellular volume fraction using routine multiphasic contrast-enhanced liver CT for staging liver fibrosis. *Clin Radiol* 72(3):242–246. doi:10.1016/j.crad.2016.10.003
 163. Silva AC, Morse BG, Hara AK, et al. (2011) Dual-energy (spectral) CT: applications in abdominal imaging. *Radiographics* 31(4):1031–1046. doi:10.1148/rg.314105159
 164. Lamb P, Sahani DV, Fuentes-Orrego JM, et al. (2015) Stratification of patients with liver fibrosis using dual-energy CT. *IEEE Trans Med Imaging* 34(3):807–815. doi:10.1109/TMI.2014.2353044
 165. Lv P, Lin X, Gao J, Chen K (2012) Spectral CT: preliminary studies in the liver cirrhosis. *Korean J Radiol* 13(4):434–442. doi:10.3348/kjr.2012.13.4.434
 166. Zhao LQ, He W, Yan B, Wang HY, Wang J (2013) The evaluation of haemodynamics in cirrhotic patients with spectral CT. *Br J Radiol* 86(1028):20130228. doi:10.1259/bjr.20130228
 167. Claudon M, Dietrich CF, Choi BI, et al. (2013) Guidelines and good clinical practice recommendations for Contrast Enhanced Ultrasound (CEUS) in the liver—update 2012: a WFUMB-EF-SUMB initiative in cooperation with representatives of AFSUMB, AIUM, ASUM, FLAUS and ICUS. *Ultrasound Med Biol* 39(2):187–210. doi:10.1016/j.ultrasmedbio.2012.09.002
 168. Ridolfi F, Abbattista T, Marini F, et al. (2007) Contrast-enhanced ultrasound to evaluate the severity of chronic hepatitis C. *Dig Liver Dis* 39(10):929–935. doi:10.1016/j.dld.2007.06.006
 169. Maruyama H, Matsutani S, Okugawa H, et al. (2006) Microbubble disappearance-time is the appropriate timing for liver-specific imaging after injection of Levovist. *Ultrasound Med Biol* 32(12):1809–1815
 170. Li N, Ding H, Fan P, et al. (2010) Intrahepatic transit time predicts liver fibrosis in patients with chronic hepatitis B: quantitative assessment with contrast-enhanced ultrasonography. *Ultrasound Med Biol* 36(7):1066–1075. doi:10.1016/j.ultrasmedbio.2010.04.012
 171. Lim AK, Taylor-Robinson SD, Patel N, et al. (2005) Hepatic vein transit times using a microbubble agent can predict disease severity non-invasively in patients with hepatitis C. *Gut* 54(1):128–133. doi:10.1136/gut.2003.030965
 172. Tang A, Kim TK, Heathcote J, et al. (2011) Does hepatic vein transit time performed with contrast-enhanced ultrasound predict the severity of hepatic fibrosis? *Ultrasound Med Biol* 37(12):1963–1969. doi:10.1016/j.ultrasmedbio.2011.09.010
 173. Barry B, Buch K, Soto JA, et al. (2014) Quantifying liver fibrosis through the application of texture analysis to diffusion weighted imaging. *Magn Reson Imaging* 32(1):84–90. doi:10.1016/j.mri.2013.04.006
 174. Vicas C, Lupsor M, Socaciu M, Nedeveschi S, Badea R (2012) Influence of expert-dependent variability over the performance of noninvasive fibrosis assessment in patients with chronic hepatitis C by means of texture analysis. *Comput Math Methods Med* 2012:346713. doi:10.1155/2012/346713
 175. Yamada H, Ebara M, Yamaguchi T, et al. (2006) A pilot approach for quantitative assessment of liver fibrosis using ultrasound: preliminary results in 79 cases. *J Hepatol* 44(1):68–75. doi:10.1016/j.jhep.2005.08.009
 176. Jirak D, Dezortova M, Taimr P, Hajek M (2002) Texture analysis of human liver. *J Magn Reson Imaging* 15(1):68–74
 177. House MJ, Bangma SJ, Thomas M, et al. (2015) Texture-based classification of liver fibrosis using MRI. *J Magn Reson Imaging* 41(2):322–328. doi:10.1002/jmri.24536
 178. Yu H, Buch K, Li B, et al. (2015) Utility of texture analysis for quantifying hepatic fibrosis on proton density MRI. *J Magn Reson Imaging* 42(5):1259–1265. doi:10.1002/jmri.24898
 179. Bahl G, Cruite I, Wolfson T, et al. (2012) Noninvasive classification of hepatic fibrosis based on texture parameters from double contrast-enhanced magnetic resonance images. *J Magn Reson Imaging* 36(5):1154–1161. doi:10.1002/jmri.23759
 180. Yokoo T, Wolfson T, Iwaisako K, et al. (2015) Evaluation of liver fibrosis using texture analysis on combined-contrast-enhanced magnetic resonance images at 3.0 T. *BioMed Res Int* 2015:387653. doi:10.1155/2015/387653
 181. Wu Z, Matsui O, Kitao A, et al. (2015) Hepatitis C related chronic liver cirrhosis: feasibility of texture analysis of MR images for classification of fibrosis stage and necroinflammatory activity grade. *PLoS ONE* 10(3):e0118297. doi:10.1371/journal.pone.0118297
 182. Kayaaltı Ö, Aksebzeci BH, Karahan İÖ, et al. (2014) Liver fibrosis staging using CT image texture analysis and soft computing. *Appl Soft Comput* 25:399–413
 183. Daginawala N, Li B, Buch K, et al. (2016) Using texture analyses of contrast enhanced CT to assess hepatic fibrosis. *Eur J Radiol* 85(3):511–517. doi:10.1016/j.ejrad.2015.12.009
 184. Zhang X, Gao X, Liu BJ, et al. (2015) Effective staging of fibrosis by the selected texture features of liver: which one is better, CT or MR imaging? *Comput Med Imaging Graph* 46(Pt 2):227–236. doi:10.1016/j.compmedimag.2015.09.003
 185. Farrar CT, DePeralta DK, Day H, et al. (2015) 3D molecular MR imaging of liver fibrosis and response to rapamycin therapy in a bile duct ligation rat model. *J Hepatol* 63(3):689–696. doi:10.1016/j.jhep.2015.04.029
 186. Fuchs BC, Wang H, Yang Y, et al. (2013) Molecular MRI of collagen to diagnose and stage liver fibrosis. *J Hepatol* 59(5):992–998. doi:10.1016/j.jhep.2013.06.026
 187. Zhu B, Wei L, Rotile N, et al. (2017) Combined magnetic resonance elastography and collagen molecular magnetic resonance imaging accurately stage liver fibrosis in a rat model. *Hepatology* 65(3):1015–1025. doi:10.1002/hep.28930
 188. Li F, Yan H, Wang J, et al. (2016) Non-invasively differentiating extent of liver fibrosis by visualizing hepatic integrin alphavbeta3 expression with an MRI modality in mice. *Biomaterials* 102:162–174. doi:10.1016/j.biomaterials.2016.06.026
 189. Hatori A, Yui J, Xie L, et al. (2015) Utility of translocator protein (18 kDa) as a molecular imaging biomarker to monitor the progression of liver fibrosis. *Sci Rep* 5:17327. doi:10.1038/srep17327
 190. Srinivasa Babu A, Wells ML, Teytelboym OM, et al. (2016) Elastography in chronic liver disease: modalities, techniques, limitations, and future directions. *Radiographics* 36(7):1987–2006. doi:10.1148/rg.2016160042